International Scientific-Technical and Production Journal

The Paton WELDING JOURNAL

March 2009 # 3

English translation of the monthly «Avtomaticheskaya Svarka» (Automatic Welding) journal published in Russian since 1948

Founders: *E.O. Paton Electric Welding Institute of the NAS of Ukraine International Association «Welding»* ***Publisher:*** *International Association «Welding»*

Address:
E.O. Paton Electric Welding Institute,
International Association «Welding»,
11, Bozhenko str., 03680, Kyiv, Ukraine
Tel.: (38044) 287 67 57
Fax: (38044) 528 04 86
E-mail: journal@paton.kiev.ua
http://www.nas.gov.ua/pwj

State Registration Certificate
KV 4790 of 09.01.2001

Subscriptions:
$324, 12 issues per year,
postage and packaging included.
Back issues available.

CONTENTS

SCIENTIFIC AND TECHNICAL

Maksymova S.V. Formation of brazed joints on titanium aluminide 2

Skulsky V.Yu. Thermokinetic peculiarities of formation of cold cracks in welded joints on hardening heat-resistant steels 8

Kuchuk-Yatsenko V.S., Shvets V.I., Sakhatsky A.G. and *Nakonechny A.A.* Features of resistance welding of titanium aluminides using nanolayered aluminium-titanium foils 11

Shonin V.A., Mashin V.S., Murashov A.P., Zelenin V.I., Demianov I.A., Pashulya M.P. and *Teplyuk V.M.* Role of protective coating of aluminium alloy welded joints in fatigue resistance 15

INDUSTRIAL

Titarenko V.I., Tkachenko O.V., Matiko D.Yu., Pilipko V.I., Mudraninets I.F. and *Mudraninets I.I.* Experience in designing and manufacture of welding-and-surfacing instalations 18

Shatan A.F., Andrianov A.A., Sidorets V.N. and *Zhernosekov A.M.* Efficiency of stabilisation of the alternating-current arc in covered-electrode welding 21

Shalomeev V.A., Tsivirko E.I., Petrik I.A. and *Lukinov V.V.* Welding repair of surface defects in Ml-10 alloy castings by using scandium-containing material 23

Litvinov A.P. Development of inert-gas welding (Review) 28

BRIEF INFORMATION

Onatskaya N.A. and *Demidenko L.Yu.* Electrohydraulic-pulsed treatment for strengthening the surfaces of 110G13MLS steel frogs 32

Thesis for a scientific degree 34

News 35

Developed at PWI 36

FORMATION OF BRAZED JOINTS ON TITANIUM ALUMINIDE

S.V. MAKSYMOVA
E.O. Paton Electric Welding Institute, NASU, Kiev, Ukraine

Studied were the features of formation of brazed joints on titanium aluminide, produced by radiation heating in vacuum using brazing filler metals based on the Ti--Zr system and alloyed with other elements. It is noted that utilisation of copper and nickel containing filler metals does not allow producing a homogeneous structure of metal of the brazed seams. Alloying the Ti--Zr system with iron, manganese and other elements provides structure and properties of the brazed seams close to those of the base material.

Keywords: *vacuum brazing, titanium aluminide, brazing filler metal, adhesion-active alloys, structure, eutectic, chemical heterogeneity*

Compositions based on the Ti--Al system are typical representatives of a new generation of high-strength and heat-resistant intermetallic alloys [1]. They hold promise for application in aircraft engineering to manufacture a number of parts of the hot section of gas turbine engines [2]. In their heat-resistant characteristics at 700--750 °C, they can compete with high-nickel alloys owing to their low specific weight [3]. This can provide a 30 % decrease in weight of a gas turbine engine.

Extensive research has been conducted in the last decades to study properties of heat-resistant titanium alloys on the intermetallic base and develop technological processes for production of permanent joints. Traditional welding methods (heating with a high heat input, application of pressure) are unacceptable in many cases.

The preferable method for joining intermetallic alloys is brazing. However, it involves a number of difficulties. On the one hand, the brazing process allows avoidance of high residual stresses in the joints, melting of the base metal and formation of cracks, as well as maintaining of mechanical properties of the base metal without violation of its structural state. On the other hand, production of brazed joints on γ-TiAl and selection of composition for brazing filler metals are limited to narrow ranges of contents of alloying elements, within which mechanical properties and performance of the base metal do not deteriorate. In this case, the rate of diffusion of many components of filler metals may be substantially slowed down because of formation of intermetallic phases with aluminium. In addition, intermetallic alloys differ in composition, and each alloy requires an individual approach to selection of filler metals and brazing temperature.

Reportedly [4, 5], components of the Ti--Al system differ much in their electronic structure of atoms and form a range of alloys, such as Ti_3Al, TiAl and $TiAl_3$. Mechanical properties of alloys based on the Ti--Al system depend upon their aluminium content. Hypostoichiometric alloys Ti--(46--49)Al (further on --- at.%), rather than single-phase γ-TiAl alloys, have maximal ductility. They belong to the two-phase $(\alpha_2 + \gamma)$-region, and the α_2-phase is represented by intermetallic Ti_3Al [4]. Alloys with the α_2-phase content of 10--15 vol.% are characterised by the maximal level of ductility [6]. Alloys with a fully lamellar coarse-grained structure (α_2 lamellae in the γ-matrix) have maximal creep resistance at increased and low temperatures.

The key drawback of the Ti--Al system based alloys under consideration, having an ordered lattice of the $L1_0$ type, is their low ductility (δ = 0.2--0.5 %) at room temperature, which is caused by specific displacement of dislocations in a face-centred tetragonal lattice. Yield stress grows with increase in temperature to about 800 °C.

So far only the first steps have been made in the field of the technology for joining intermetallic alloys by brazing. Criteria for selection of this joining method or the other have not been developed as yet. In this connection, we can speak only about individual studies. Moreover, these studies do not always answer the main goal, which consists in providing high performance of the joints under service conditions.

Vacuum brazing [7] of intermetallic titanium alloy Ti--37.5 % Al, whose structure is represented by the lamellar γ(TiAl)- and $\alpha_2(Ti_3Al)$-phases, is performed by using the 15 μm thick aluminium foil, and by applying a compressive force and holding at a temperature of 700 or 900 °C, this favouring the diffusion processes and formation of intermetallics $TiAl_2$ (or $TiAl_3$) in the brazed seam metal. Long-time heat treatment of the brazed joints at 1300 °C with holding for 3.84 ks failed to provide formation of the lamellar γ/α_2-phase and strength of the brazed joints at a level of the base metal. Tensile strength σ_t at a temperature of 20 °C was approximately 220 MPa [7]. A drawback of this technological process is that it is labour- and time consuming. In addition, application of the compressive force is determined by design features of a specific brazed part. Hence, it cannot be considered a versatile method for production of permanent joints.

In the case of vacuum brazing at a temperature of 990 °C for 30 min, the use of silver as a brazing filler metal did not provide serviceable joints, as there was no diffusion of elements of the base metal into the seam and silver into the base metal. Defects in the form of pores were found in the brazed seam. The use of alloy based on the Cu--Ni system as a brazing filler metal did not give positive results either [8].

Strength of the brazed joints was increased to 343 MPa owing to the use of silver filler metal BAg-8 [9]. It was noted that silver does not enter into reaction with TiAl (base metal) [9], whereas copper, on the contrary, actively interacts with it. For example, phases of the AlCuTi and $(AlCu)_2Ti$ types formed at interface between the filler and base metals at a brazing temperature of 950 °C. The rate of growth of the first phase was much higher, compared with that of the second phase. It should be noted that intermetallic titanium alloys TiAl are intended for operation at increased temperatures. Therefore, the use of silver filler metals is not indicated in view of increased requirements to heat resistance.

Alloy Ti--48Al--2Cr--2Nb is a classic example of intermetallic titanium alloys. The main structural component of this alloy is an ordered γ-phase (TiAl), along the boundaries of which an insignificant amount of the α_2-phase (Ti_3Al) precipitates in the form of lamellar grains. Owing to this lamellar microstructure this alloy features a good balance between ductility and strength at increased temperatures (Figure 1), as well as oxidation resistance [10]. Diffusion brazing of this alloy [11] was carried out by using 5 and 50 μm thick foils of pure copper and billets of composite embedded elements of alloy TiAl--Cu (in brazing with a wide gap).

It was shown that the seam metal with a structure close to that of the base metal can be produced in both cases after a short time of brazing and subsequent heat treatment [11]. Utilisation of traditional 50 μm thick embedded elements (copper) leads to increase in the brazing time. However, it does not provide a sufficient value of shear strength. Strength of the brazed joints increases to some extent (250 MPa), although not reaching the level of the base metal, in brazing with a wide gap (350--500 μm) by using 5 μm thick copper foils or composite interlayers of alloy TiAl--Cu.

Analysis of the above studies allowed a conclusion that production of the brazed joints on intermetallic titanium alloys requires that long-time holding be used in brazing (or heat treatment). However, even sophisticated and long-time technological processes used to produce permanent brazed joints fail to provide their strength equal to that of the base metal.

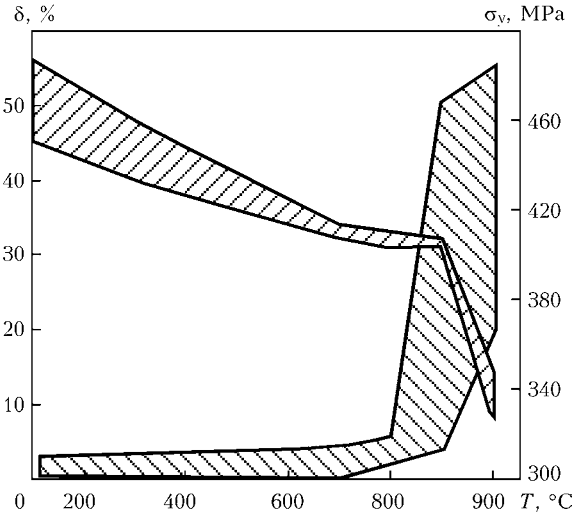

Figure 1. Variations in mechanical properties (ductility δ and yield stress σ_y) of alloy Ti--48Al--2Cr--2Nb with temperature

This study was conducted on intermetallic alloy Ti--45Al--2Nb--2Mn + 0.8 vol.% TiB_2, which in the initial state (as-delivered) is characterised by the presence of a lamellar structure. An insignificant amount of the α_2-phase (Ti_3Al) of a light plate-like type precipitates along the boundaries of the main structural component, i.e. ordered γ-phase (TiAl) (Figure 2). Needle-shaped borides 1 μm wide and up to 30 μm long are occasionally found. Their boron content amounts to 75 %, which is confirmed by the results of examination of chemical heterogeneity of the alloy (Table 1). It should be noted that the alloy was produced by the powder metallurgy method, and is characterised by the presence of porosity, which makes the brazing process more difficult to perform.

To achieve good wetting of the base material and optimal properties of the brazed joints, a chemical element, which is the main element of the base material, is usually chosen as a base of a brazing filler metal. Chemical elements of the brazing filler metal

Table 1. Content of chemical elements in local regions of alloy Ti--45Al--2Nb--2Mn + 0.8 vol.% TiB_2

Investigated region (spectrum)	Ti	Al	Mn	Nb	B
1	48.00	48.65	1.51	1.85	0
2	53.25	42.74	1.94	2.07	0
3	18.52	5.54	0.18	0.74	75.02
4	22.18	7.04	0.29	0.82	69.67

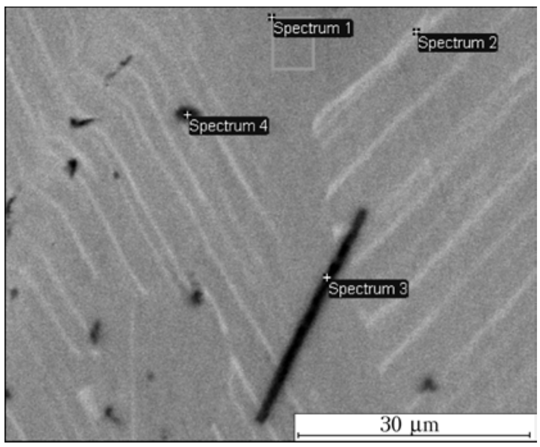

Figure 2. Microstructure of intermetallic alloy Ti--45Al--2Nb--2Mn + 0.8 vol.% TiB_2

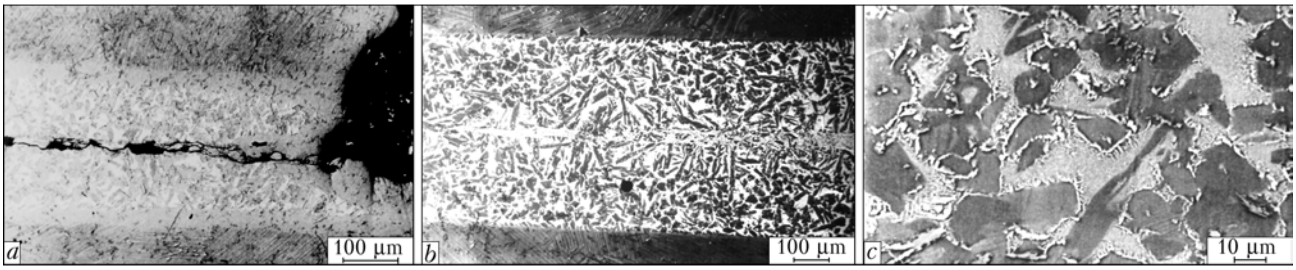

Figure 3. Microstructure of metal of the brazed joint produced by using commercial filler metal Ti--7.31Zr--20.06Cu--11.3Ni: *a* ---- crack; *b, c* ---- eutectic and structure of the central part of the seam

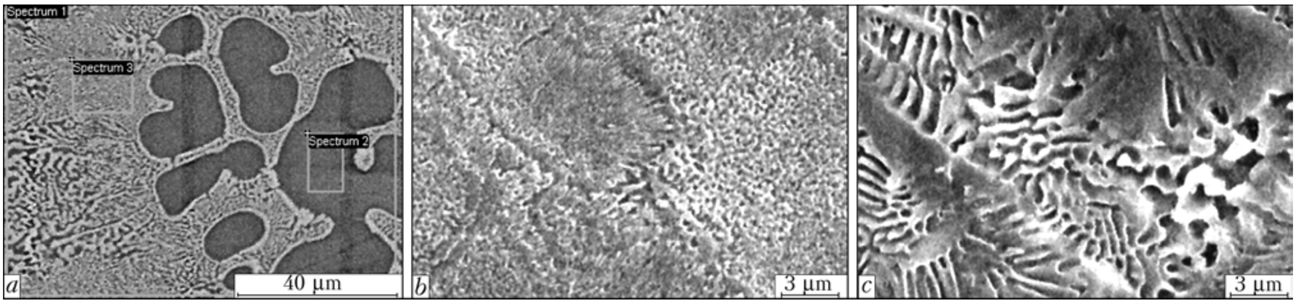

Figure 4. Microstructure of filler metal Ti--30Zr--25Fe in the cast form (see explanations in the text)

should have such a temperature range which would suit a specific base material, do not deteriorate its properties and provide formation of chemical compounds with the base metal. Titanium foils and alloys of the following systems: Ti--30Zr--25Cr (*A*), Ti--30Hf--25Fe (*B*), Ti--30Zr--25Fe (*C*), Ti--30Zr--*x*Mn (*D*) ($x = 0$--40 % Mn) and Ti--7.31Zr--20.06Cu--11.3Ni (*E*), were tested as brazing filler metals.

Zonal chemical heterogeneity was detected in the brazed seams at a brazing temperature of 1250 °C (for 60 min) when using commercial filler metal Ti--7.31Zr--20.06Cu--11.3Ni (*E*). Eutectic, acting as a centre of initiation and propagation of cracks (Figure 3, *a, b*) and deteriorating mechanical properties of the brazed joints, solidifies, as a rule, along the seam axis and in fillet regions. Grains of a faceted shape crystallise in structure of the central part of a specimen against a background of the light eutectic network. The aluminium content of these grains is 36.34 %, this corresponding to compound $TiAl_2$. The grains are fringed with a light phase, the content of which is impossible to determine because of its small size (Figure 3, *c*). Therefore, structure of the brazed seam metal consists of three phase components. These structural peculiarities are characteristic only of the brazed joints produced by using commercial filler metal *E*.

Table 2. Content of chemical elements in local regions of cast alloy Ti--30Zr--25Fe

Investigated region (spectrum)	Ti	Zr	Fe
1	63.05	18.34	18.61
2	73.79	15.33	10.88
3	56.56	20.09	23.36

The attractive feature of utilisation of adhesion-active alloys based on the Ti--Zr system as brazing filler metals is that this system is characterised by the presence of a continuous series of solid solutions over the entire range of concentrations. It might be expected that the above peculiarity of alloys of this system would have a positive effect on properties of the brazed joints on titanium alloys. In addition, the use of the adhesion-active elements leads to improvement of wetting of the substrate to be brazed. Adding other elements to alloys of the Ti--Zr system made it possible to substantially decrease their melting point due to formation of low-melting point eutectics. Alloys of the Ti--Zr--Mn and Ti--Zr--Fe systems hold promise for development of brazing filler metals. Relatively low-melting point eutectics (melting point 1180, 1085, 1135 and 928 °C) form in binary systems Ti--Mn, Ti--Fe, Zr--Mn and Zr--Fe between the β(Ti) and β(Zr) solid solutions and titanium- and zirconium-rich intermetallics [4, 12--14].

Typical eutectic microstructure is shown in Figure 4, *a*--*c*, by an example of cast alloy Ti--30Zr--25Fe. First the primary dendrites of the titanium-base solid solution solidify in cooling of a liquid alloy (spectrum 2 in Table 2; Figure 4, *a*), then follows nucleation, growth and formation of rod-shaped eutectic colonies (spectrum 3 in Table 2; Figure 4, *b*). The average content of zirconium in the eutectic is 20.09 % (Table 2). Detailed investigations of morphological peculiarities and chemical composition of structural components of the eutectic showed that both phases contained zirconium, its content being maximal in the light phase (24.81 %). Assumingly, this is a zirconium intermetallic, and it is the main phase in solidification of the alloy. The second phase is a solid solution containing more titanium (67.93 %) and less zirconium (16.45 %). Morphological structure of this eutectic is characterised by an ordered arrangement of the com-

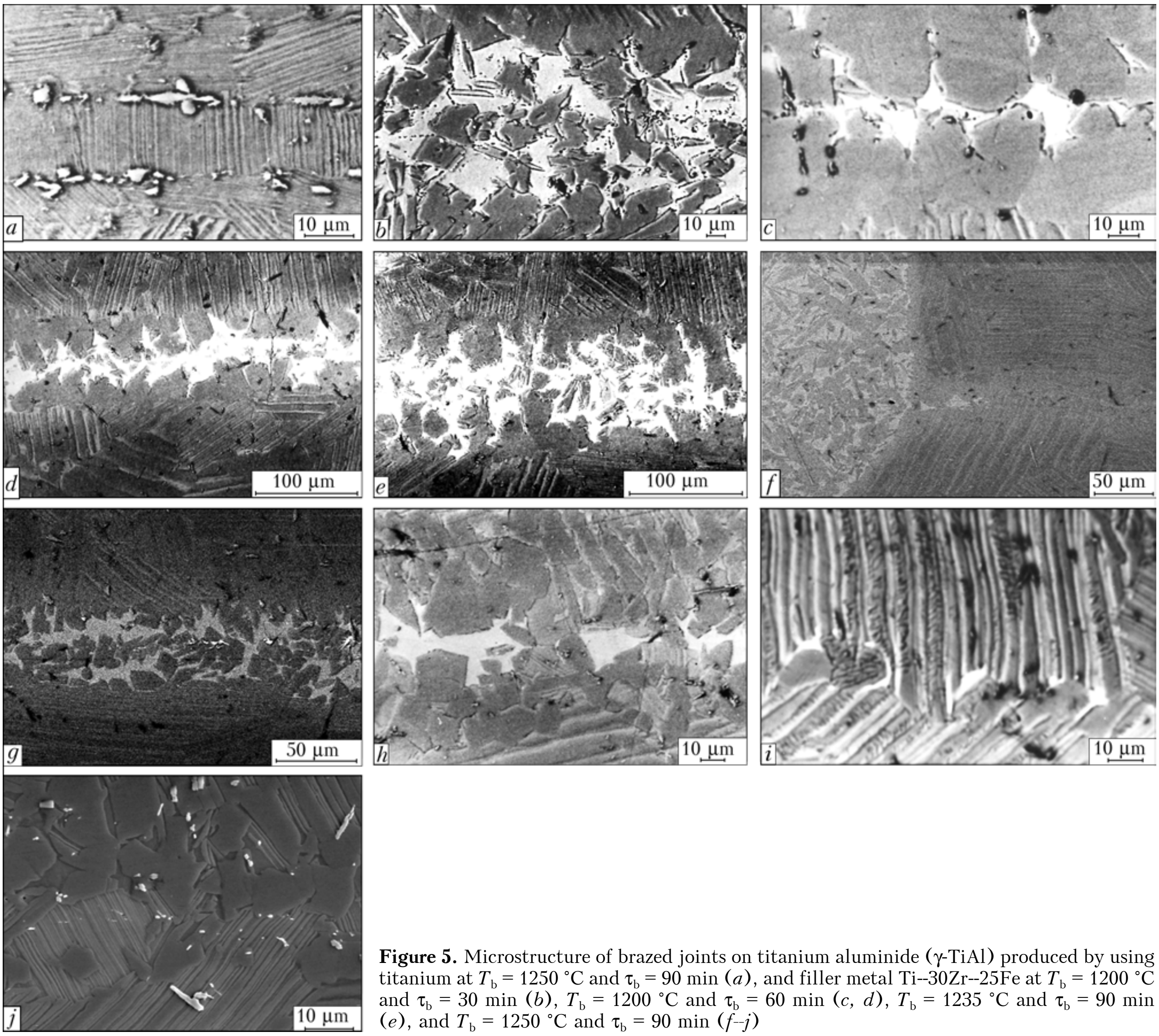

Figure 5. Microstructure of brazed joints on titanium aluminide (γ-TiAl) produced by using titanium at T_b = 1250 °C and τ_b = 90 min (*a*), and filler metal Ti–30Zr–25Fe at T_b = 1200 °C and τ_b = 30 min (*b*), T_b = 1200 °C and τ_b = 60 min (*c, d*), T_b = 1235 °C and τ_b = 90 min (*e*), and T_b = 1250 °C and τ_b = 90 min (*f–j*)

ponent phases in the form of rods. According to the Scheil classification of eutectics [15], this type of the eutectics is classed with normal eutectics having a cellular sub-structure (Figure 4, *b*). They may be of the other types, depending upon the cooling rate, e.g. skeleton type (Figure 4, *c*), where grains of the eutectic phases making up a colony grow in the form of fine branched dendrites. Such structural peculiarities of alloy Ti–30Zr–25Fe have no impact on properties of the brazed joints.

Intermetallic titanium alloy can be well wetted by eutectic alloys based on the Ti–Zr system. Face and reverse fillets are formed in the brazed joints. Metallography and investigation of chemical heterogeneity of overlap brazed joints show that the diffusion processes occur actively between the base metal and liquid filler metal. During brazing, aluminium diffuses from the base into seam metal. The brazed seam, where the aluminium content corresponds to that of the base metal, forms even in the case of using a titanium foil 0.01 mm thick (temperature T_b = 1250 °C and time τ_b = 90 min). The titanium-base phase of a discrete type, containing 11.28 Al, solidifies at interface with the base metal (Figure 5, *a*). According to the constitutional diagram of Ti–Al, this composition is characteristic of the α-phase (solid solution of aluminium in titanium).

Vacuum brazing of overlap joints on titanium aluminide by using filler metal Ti–30Zr–25Fe provides tight seams with a face and reverse fillets, the base metal retaining its lamellar structure (Figure 5, *b–f*). Fillet regions and wide seams contain two phases (Figure 5, *f–h*). As a result of the diffusion processes occurring at the base metal–liquid fillers metal interface, a dark phase solidifies in the fillet region along the interface, having the form of a solid band and separate grains in the bulk of the molten filler metal, and containing 43 % Al (filler metal *C*). The aluminium content of the light matrix is lower (31 %) (Figure 5, *f*). The process of solidification of brazed seams has its own peculiarities caused by the presence of small gaps, non-equilibrium solidification conditions, base metal substrate, and gradient of concentrations of chemical elements making up the filler and base metals. Oversaturation of the seam metal with aluminium occurs with time, this causing nucleation

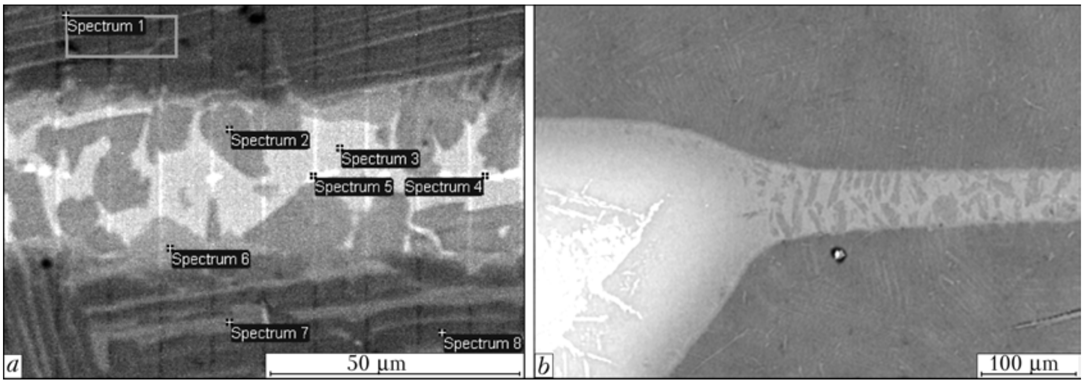

Figure 6. Microstructure of metal of brazed joint (*a*) and fillet region (*b*) produced by using filler metal of the Ti--Zr--Cr system

and growth of primary crystals of the γ-TiAl phase in the form of dark grains both on the base metal substrate and in the bulk of the melt at the seam centre (Figure 5, *g, h*). The α_2-Ti_3Al phase solidifies later. It fills up the space between the TiAl crystals and contains 32 % Al (Figure 5, *b--d*). Width of the seam is a variable that depends upon many parameters, such as width of the brazing gap, amount of the filler metal, brazing temperature, holding time and rate of dissolution of the base metal. There are regions with a seam width of 50 and 20 μm (Figure 5, *g, h*). Also, the joint comprises regions where there is no seam as it is, but where there are coalesced grains of the base metal with an aluminium content increased to 46 %, which is identical to the base metal. The seam metal is characterised mostly by the lamellar structure, close to that of the base metal (Figure 5, *i, j*). Chemical composition of the seam metal is determined by the processes occurring at the solid metal--liquid filler metal interface. Hence, it is substantially different from that of the filler metal in the initial state.

The diffusion processes take place in the seam metal even at τ_b = 5 min and T_b = 1180 °C when using filler metal of the Ti--Zr--Cr system, which is proved by the results of investigation of chemical heterogeneity (Table 3). The content of aluminium in the base metal (in the zone adjoining the seam) and in the dark grains of the seam metal (TiAl phase) is approximately identical (42.14--43.55 %). As follows from the above-said, grains of the TiAl phase (spectra 2 and 6 in Table 3; Figure 6, *a*) located in the seam metal have a maximal aluminium content. They form both on the base metal substrate (Figure 6) and in the central part of the seam, an insignificant amount of elements of the base metal being revealed in their composition. These peculiarities of formation of the seams are characteristic only of the brazed joints produced by using experimental alloys of the Ti--Zr system. Distinctive feature of the seam when using the Ti--Zr system alloy is that its central part contains dispersed phase precipitates in the form of very fine individual spots or plates enriched with zirconium (spectra 4 and 5 in Table 3; Figure 6, *a*).

The phase containing 32--37 % Al solidifies in the fillet region located along the interface with the base metal. The central part of this region contains eutectic

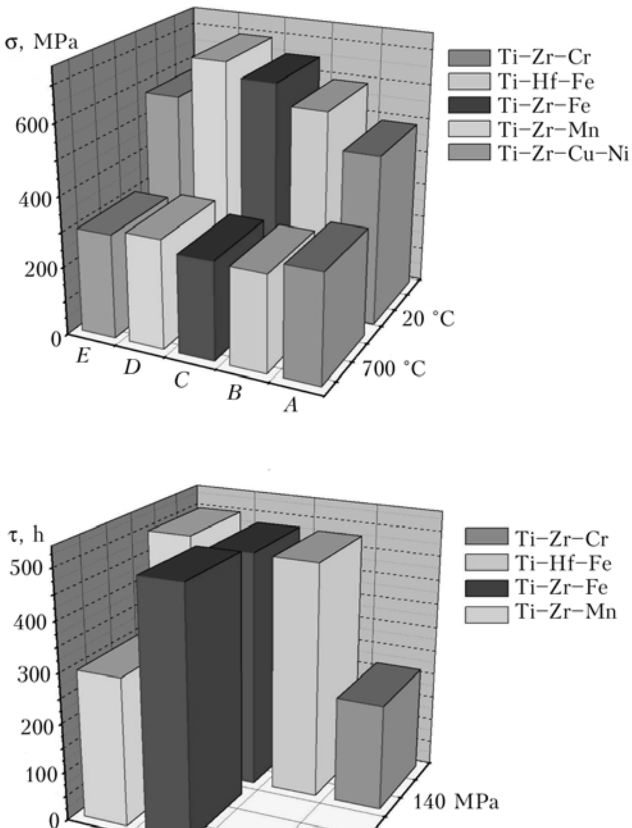

Figure 7. Mechanical properties of brazed joints: *a* ---- short-time tensile strength σ at *T* = 20 and 700 °C; *b* ---- long-time strength at *T* = 700 °C and load of 140 and 200 MPa

Table 3. Content of chemical elements in brazed joint metal

Investigated region (spectrum)	Al	Ti	Cr	Mn	Zr	Nb
1	42.14	55.21	--	0.71	--	1.94
2	43.55	49.14	1.43	0.54	3.60	1.75
3	32.20	56.83	4.45	1.70	2.83	2.00
4	32.64	52.07	2.51	0.63	10.97	1.17
5	33.40	51.68	2.50	0.55	10.82	1.05
6	37.55	55.71	1.69	0.80	2.21	2.04
7	37.96	58.72	--	1.12	--	2.19
8	43.88	53.09	--	0.94	--	2.09

with a lower aluminium content and higher zirconium content.

It should be noted that in the case of using filler metals of the Ti–Zr system the zirconium content of the seam metal decreases with increase in holding time at a brazing temperature, this being caused by mutual solubility in the Ti–Zr system [3]. The fillet regions contain more liquid filler metal than the seams. Length of the contact line between the filler and base metals is smaller, and the diffusion processes are less efficient. Therefore, the fillet regions contain more zirconium than the seam metal. The TiAl phase solidifies in the form of a narrow continuous band (about 25 μm wide) located along the base metal.

Analysis of the results shows that brazing of intermetallic alloy γ-TiAl using filler metals of the Ti--Zr system leads to substantial enrichment of the seam metal with aluminium, i.e. its content is the same as in the TiAl and Ti_3Al phases. Utilisation of filler metals of the Ti--Zr--Fe (*C*) and Ti--Zr--Mn (*D*) systems provides formation of sound defect-free seams, which contain no eutectic component. Results of mechanical tests at room temperature showed that specimens produced by using the *C* and *D* filler metals had a maximal value of short-time strength (Figure 7, *a*). Strength of the brazed joints remained almost unchanged with increase in temperature to 700 °C. It was established that brazed joints produced by using filler metal Ti–Zr--Cr (*A*) exhibited a minimal strength in long-time strength tests at a temperature of 700 °C and load of 140 MPa (Figure 7, *a*). Specimens of these joints fractured in the brazed seam, whereas specimens produced by using the *D* and *C* filler metals did not fracture not only at the preset (140 MPa) but also increased (200 MPa) load (Figure 7, *b*).

CONCLUSIONS

1. Zonal chemical heterogeneity and solidification of three phase components, such as eutectic and two titanium-base phases differing in the aluminium content, take place in the seam metal produced by brazing titanium aluminide Ti--45Al--2Nb--2Mn + 0.8 vol.% TiB_2 using a filler metal based on the Ti--Cu--Zr--Ni system.

2. Utilisation of adhesion-active filler metals based on the Ti–Zr system allowed avoidance of formation of the eutectic component and provided the brazed seams with a two-phase structure, i.e. TiAl and Ti_3Al, which is characteristic of the base metal.

3. Filler metals based on the Ti--Zr--Fe and Ti–Zr–Mn systems provided maximal values of short- and long-time strength of the brazed joints.

1. Kablov, E.N. (2003) VIAM ---- the heart of aircraft materials science. *Vestnik Vozdushn. Flota*, **4**, 6.
2. Bochvar, G.A., Salenkov, V.S. (2004) Study of titanium aluminide based alloy with orthorhombic structure. *Tekhnologiya Lyog. Splavov*, **4**, 44--46.
3. Kolachev, B.A., Livanov, V.A., Elagin, V.I. (1981) *Metals science and heat treatment of nonferrous metals and alloys*. Moscow: Metallurgiya.
4. (1999) *Constitutional diagrams of binary metal systems*: Refer. Book. Ed. by N.P. Lyakishev. Vol. 3, Book 1. Moscow: Mashinostroenie.
5. (1990) *Binary alloy phase diagrams*. Ed. by T.V. Massalski. Ohio: ASM Int., Materials Park.
6. Bannykh, O.A., Povarov, K.B., Braslavskaya, G.S. et al. (1996) Mechanical properties of cast γ-TiAl alloys. *Metallovedenie i Term. Obrab. Metallov*, **4**, 11--14.
7. Uenishi Keisuke, Sumi Hiroyuki, Kobayashi Kojiro. (1995) Joining of intermetallic compound TiAl by using Al filler metal. *Z. Metallik.*, 86(**4**), 270--274.
8. Xu, Q., Chaturvedi, M.C., Richards, N.L. et al. (2000) Diffusion brazing of TiAl alloy. In: *Proc. of Int. Brazing & Soldering Conf.* (April 2--5, 2000, Albuquerque, New Mexico). Ohio: ASM Int., Materials Park, 57--64.
9. Chen, S.Y., Wu, S.K., Shiue, R.K. (2003) Infrared brazing of TiAl intermetallic using Bg-8 braze alloy. *Acta Mater.*, 51(**77**), 1991--2004.
10. Helmut, C. (1995) Intermetallic γ-TiAl based alloy sheet materials. *Zeitschrift fuer Metallkunde*, 86(**12**), 814--822.
11. Gale, W.F., Wen, X. Shen, Y. et al. (2000) Diffusion brazing of titanium aluminide ---- wettability, microstructural development and mechanical properties. In: *Proc. of Int. Conf. on Brazing & Soldering*. (April 2--5, 2000, Albuquerque, New Mexico). Ohio: ASM Int., Materials Park, 42--49.
12. Khorunov, V.F., Maksymova, S.V., Ivanchenko, V.G. (2004) Production of brazed joints on γ-TiAl and study of their properties. *Adgeziya Rasplavov i Pajka Materialov*, **37**, 88--95.
13. Khorunov, V.F., Maksymova, S.V. (2007) Structure and properties of intermetallic alloy brazed joints. In: *Proc. of National Welding Conf.* (China, Hefei, Oct. 2007), 348--352.
14. Khorunov, V.F., Maksymova, S.V. (2000) Intermetallic alloy γ-TiAl brazing. In: *Proc. of 3rd Int. Brazing and Soldering Conf.* (USA, San Antonio, Texas, 2006). Ohio: ASM Int., Materials Park, 288--292.
15. Taran, Yu.N., Mazur, V.I. (1978) *Structure of eutectic alloys*. Moscow: Metallurgiya.

THERMOKINETIC PECULIARITIES OF FORMATION OF COLD CRACKS IN WELDED JOINTS ON HARDENING HEAT-RESISTANT STEELS

V.Yu. SKULSKY
E.O. Paton Electric Welding Institute, NASU, Kiev, Ukraine

Crack resistance of welded samples of steels with martensite and martensite-bainite transformations under isothermal conditions at different heating temperatures was studied by using the «Implant» testing machine equipped with the automatic heating and temperature monitoring system. It is shown that the risk of cold cracking of welded joints on martensitic steels is run in cooling after welding, starting from temperatures of 140--120 °C. The welded joints on steel with the bainitic-martensitic structure become sensitive to cracking at a temperature below 80 °C.

Keywords: *arc welding, heat-resistant steels, welded joints, cold cracks, delayed fracture, temperature effect, structure, martensite, bainite*

Cold cracks initiate and propagate in welded joints on modern multi-component heat-resistant steels with a relatively low content of carbon (~0.08--0.12 %) during a certain period of time, i.e. their formation is of a delayed character. As determined in numerous studies, the delayed fracture is a result of the loss of strength of atomic bonds in a quenched metal under the effect of hydrogen, as well as the presence of stresses sufficient for fracture (structural stresses forming as a result of quenching, and welding stresses developing in cooling of a joint) [1--9]. The initial stage of the delayed fracture is a local microplastic deformation, which forms under the effect of stresses in the zones that are more sensitive to movement of dislocations (normally, near the grain boundaries). Capture of diffusible hydrogen in the form of protons by dislocations and its transportation by the dislocations into their accumulation zone near the barriers, which are, in particular, the high-angle boundaries, lead to formation of a local critical state (limiting concentration of hydrogen and density of dislocations), at which the embryos of a future crack initiate. As a result, the hydrogen induced cracks propagate along the grain boundaries and, in some cases, along the sub-boundaries in the bulk of grains.

Despite a large number of studies dedicated to the problem of cold cracks, which confirm the considered regularities of the delayed fracture, it is necessary to clarify some points of the mechanism of this phenomenon. In particular, peculiarities of the effect of temperature on the sensitivity to cold cracking are little studied. The temperature, at which the welded joints show their sensitivity to the delayed fracture, as given in literature sources, is insufficiently accurate. For example, according to different data, the cracks may form at temperatures of 300 °C and lower [10], 200 °C and lower [11, 12], below 130 °C [11], below 120--150 °C [12], at 100 °C and lower [13, 14], at 50--70 °C [14], and at room temperature [11--15]. At the same time, a more precise definition of the temperature, below which the risk of cracking is run, is of a practical importance. In some cases, when using hard-to-weld steels, it is reasonable to start heating for tempering of the welded joints not waiting for their cooling below a dangerous temperature limit (e.g., below 100 °C for the joints on martensitic steel of the 20Kh12MF type).

The purpose of this study was to investigate thermokinetic peculiarities of formation of cold cracks, as well as estimate the limiting temperature (in a range below the phase transformation temperature), at which the welded joints on hardening steels show the sensitivity to the delayed fracture during cooling.

The known «Implant» method was employed to investigate the crack resistance [16, 17]. Steels that harden to form the martensitic (P91 (of the 10Kh9MFB type), 25Kh2NMFA, 38KhN3MFA) and bainitic-martensitic structure (10GN2MFA) were used for making the cylindrical implant samples welded to a plate to simulate the experimental joints. Electrodes FOX C9MV were used to produce joints on steels 10Kh9MFB and 25Kh2NMFA, experimental electrodes providing identical alloying of the deposited metal were used for steel 38KhN3MFA, and electrodes TML-3U were used for steel 10GN2MFA. Fracture occurred in a hardened HAZ metal during testing. To initiate fracture, the samples had on their surfaces a stress raiser of the V-shaped profile, made in the form of a spiral. The tests were conducted by maintaining a constant temperature within the zone of a welded joint. To do this, resistance heater *2* (Figure 1) connected to electronic regulator *1* for automatic monitoring of a temperature and switching on of heating was placed on plate *3* with an experimental joint. Thermocouple *7* of the KhA type, passing through a hole drilled in the plate and welded (by using the capacitor-discharge machine) to sample *4* in the HAZ region was used to measure the temperature. Automatic heating was switched on when a sample cooled down after welding to a temperature set by control unit *1*. The tests were performed at temperatures rang-

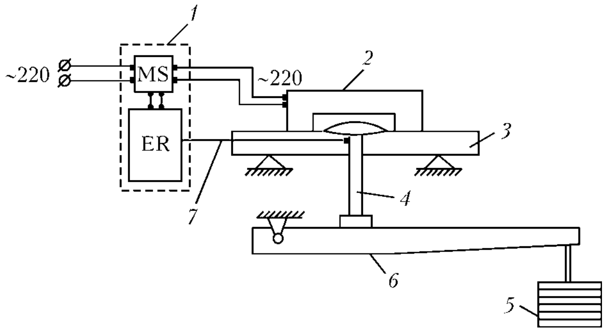

Figure 1. Schematic diagram of «Implant» test with heating of a welded joint: *1* ---- heating control unit (ER ---- electronic temperature regulator, MS ---- magnetic starter); *2* ---- heater; *3* ---- plate; *4* ---- sample (Implant); *5* ---- set of weights; *6* ---- lever; *7* ---- thermocouple

ing from the ambient one (~20 °C) to a temperature at which the sensitivity to cracking was absent. A set of replaceable weights *5* connected to lever *6* of the machine was employed to load the welded joints.

The experimental results are shown in Figures 2--4. As follows from these results, the welded joints on low-carbon martensitic steels of the 10Kh9MFB type start exhibiting the sensitivity to the delayed fracture at a temperature of about 140 °C and lower (Figure 2). The level of the upper temperature limit of appearance of the sensitivity to cracking lowers with decrease in external loading macrostresses in a welded joint, and varies from 140 to 120 °C. This temperature region can be considered transitional from a region of no sensitivity to cold cracking (at $T > 140$ °C) to a region of a potential sensitivity to cold cracking (at $T < 120$ °C). The welded joints had a minimal crack resistance at temperatures of about 100--80 °C, this corresponding to a minimal time of development of the fracture. At lower temperatures, the time of the process of the delayed fracture grows.

Hardened metal exhibits the sensitivity to loading macrostresses in all the cases. Increase in these stresses leads to growth of the degree of the general stress-strain state (total effect of micro- and macrostresses) and accelerated fracture.

Crack resistance of the welded joints on steels 25Kh2NMFA and 38KhN3MFA varied in a similar manner (Figures 3 and 4). The general peculiarities of development of the delayed fracture, except for some differences, include: absence of the sensitivity

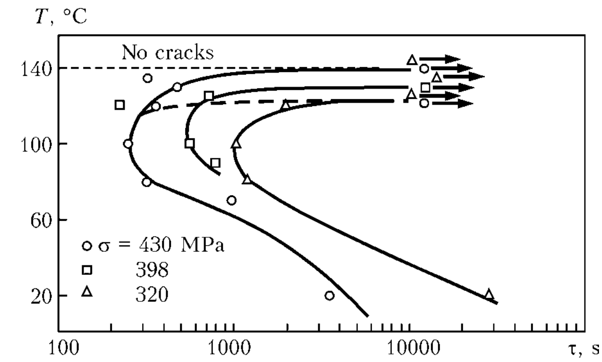

Figure 2. Effect of temperature and stresses on time of delayed fracture of welded joints on martensitic steel 10Kh9MFB (of the P91 type)

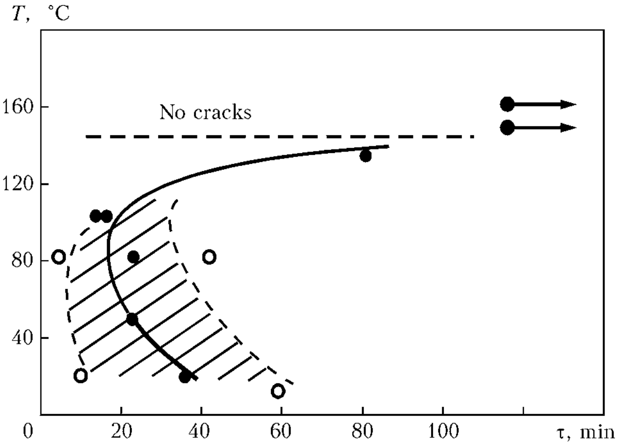

Figure 3. Effect of temperature on time of delayed fracture of welded joints on martensitic steel 25Kh2NMFA (σ = 400 MPa)

to cracking at temperatures above 130--140 °C, cracking depending upon the level of effective stresses develops at temperatures below 140 °C, state with a minimal crack resistance occurs at temperatures from 100 to 80 °C, and time of fracture grows at room temperatures.

As shown by the experiments, the welded joints on steel 38KhN3MFA had a high sensitivity to the applied stresses. The fracture occurred much quicker and at lower loading stresses, compared with the joints on steel with 9 % Cr. In this case the microstresses forming during phase hardening in alloyed steel 38KhN3MFA with an increased content of carbon had

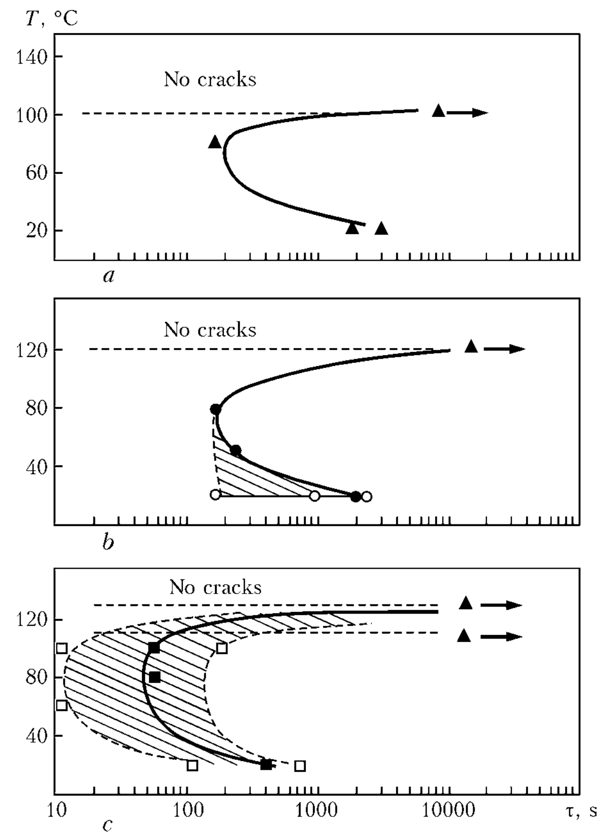

Figure 4. Effect of temperature and loading stresses on variation in time of delayed fracture of welded joints on martensitic steel 38KhN3MFA: *a* ---- σ = 170 MPa; *b* ---- 218; *c* ---- 290

a higher effect. As a result, it was enough to apply lower stresses to initiate cracking.

Phase hardening is known to be caused by development of differently directed microshear strains in the bulk of metal as a result of non-equilibrium (martensitic) transformation of overcooled austenite. Partial tempering (sometimes called self-tempering) of martensite may have time to occur to this degree or the other at a stage of further cooling, depending upon the transformation temperature M_s, which causes some increase in ductility of this martensite. Stability of austenite under overcooling conditions grows with increase in the degree of alloying of metal, especially with increase in the carbon content, which leads to lowering of temperature M_s. This results in increase of the degree of hardening of hardened martensite (the measure of which can be hardness), and in deterioration of weldability. Transformation of low-hardened austenite in low-carbon materials with a low content of alloying elements occurs at a relatively high temperature, at which a partial development of equilibrium $\gamma \rightarrow \alpha$ transformation, in addition to the martensite one, may take place. Self-tempering of microregions may reach a high degree in cooling of such a metal. Under such conditions, which are characteristic of formation of the martensitic-bainitic structure, the metal acquires a lower hardening degree than in the case of formation of the purely martensitic structure at a lower temperature. The above regularities tell on the properties of the steels under investigation, which are characterised by the following temperatures of beginning of martensite transformation and values of hardness in the hardened state: 10GH2MFA — M_s = = 430 °C/*HV* 380, 25KhN3MFA — 375 °C/*HV* 450, 10Kh9MFB (P91) — 380 °C/*HV* 450, and 38KhN3MFA — 300 °C/*HV* 600.

In addition, the role of a structural factor in manifestation of a different sensitivity to cracking by the hardened metal has the following peculiarities. Cold-hardening in deformation is known to be accompanied by an increased quantity of dislocations in metal. The dislocation density equal to 10^{15}–10^{16} m^{-2} is critical. Exceeding the above values as a result of extra deformation leads to fracture of polycrystalline materials [18]. Phase hardening in martensite transformation is accompanied by formation of the dislocation density of the same order of magnitude (10^{11}–10^{12} cm^{-2}) [19, 20]. Therefore, the martensite transformation brings metal closer to the pre-fracture state. As dislocations have a non-uniform distribution (there are regions with a high and low dislocation density), the metal may be characterised, depending upon the initial degree of hardening, by a certain safety factor for ductility and have a compliance for development of local deformation before initiation of fracture. That is why the low-carbon martensitic metal also requires some additional plastic deformation to reach the critical dislocation density in some microregion for a crack to initiate. At the presence of hydrogen the fracture initiates at a lower dislocation density than the critical one, characteristic of a heavily deformed metal. This state in our experiments was achieved by using an external load. Martensite in a metal with high carbon content, because of higher tetragonality of the crystalline lattice and higher hardening degree, acquires higher rigidity at a dislocation density that is even more close to the critical one. Seemingly, this is the reason why microdeformation under the effect of stresses is of a more concentrated character in a strongly hardened metal with an increased rigidity of the matrix than in a less hardened low-carbon martensitic metal, and why lower applied stresses and initial strain suffice for cracking.

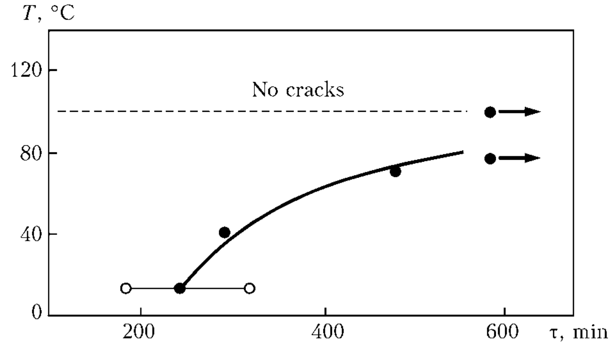

Figure 5. Effect of temperature on time of delayed fracture of welded joints on steel 10GN2MFA (σ = 320 MPa)

Metal of the welded joints with the bainitic-martensitic or bainitic structure has higher resistance to the delayed fracture because of a lower degree of hardening. As seen from Figure 5, the joints on steel 10GN2MFA become sensitive to cracking at a temperature below 80 °C. However, the structural heterogeneity, which is related to formation of martensite-like rigid microzones and less strong ferritic microregions, may be a negative factor that deteriorates to some extent the crack resistance of metal with the bainite transformation. The probability of easy development of the concentrated deformation in softer components of a microstructure facilitates initiation and propagation of cracks [9]. In general, judging from the experimental observations, the welded joints with the bainitic-martensitic or bainitic structure are characterised by a better weldability than those with the martensitic structure.

Based on the existing notions of the micromechanism of development of the delayed fracture, it can be suggested that the revealed temperature dependence of the sensitivity to cracking is related to a structural state, which determines the character of development of the initial microplastic deformation under the effect of stresses, as well as the speed of reaching the critical concentrations of dislocations and hydrogen in some microregions, which are sufficient for initiation of fracture.

Therefore, it was established as a result of «Implant» tests of the samples of steel 10Kh9MFB conducted at different temperatures that the sensitivity of the welded joints on martensitic steels to cold cracking at a stage of cooling after phase transformation starts showing up at a temperature of 140 °C and lower. The level of the upper temperature limit depends upon the general stress-strain state of metal of a welded joint, and varies approximately from 140 to 120 °C. Below 120 °C, the welded joints become potentially sensitive to cracking. At a temperature of 100 to 80 °C, the welded joints on martensitic steels have a minimal cold crack resistance, which shows up in a minimal time of development of the delayed fracture. The time of fracture increases with decrease in temperature.

The similar dependence of crack resistance upon the temperature persists in the welded joints on hard-to-weld martensitic steels with an increased content of carbon, which was demonstrated by an example of steel 38KhN3MFA. However, growth of the degree of hardening of martensite in quenching as a result of increased alloying of the steel with carbon (as well as with other elements) leads to increase in the sensitivity of the welded joints on such steel to microstresses, especially in the presence of stress raisers, and to a substantial decrease in cold crack resistance.

Tests of the samples of steel 10GN2MFA showed that the welded joints with the bainitic-martensitic structure and a lower degree of hardening in welding are characterised by a higher crack resistance than the joints on martensitic steels. The sensitivity of the welded joints with the bainitic-martensitic structure to the delayed fracture shows up at a temperature of 80 °C and lower.

1. Kasatkin, B.S., Musiyachenko, V.F. (1974) Mechanism of formation of intercrystalline cold cracks in near-weld zone of tempered steel welded joint. *Problemy Prochnosti*, **10**, 3--9.
2. Kasatkin, B.S., Brednev, V.I. (1985) Peculiarities of the process of cold cracking in welded joints on low-alloy high-strength steels. *Avtomatich. Svarka*, **8**, 1--5, 18.
3. Kasatkin, O.G. (1994) Peculiarities of hydrogen-induced embrittlement of high-strength steels in welding. *Ibid.*, **1**, 3--7.
4. Kasatkin, B.S., Smiyan, O.D., Mikhajlov, V.E. et al. (1986) Effect of hydrogen on sensitivity to cracking in HAZ with stress concentrators. *Ibid.*, **11**, 20--23.
5. Kasatkin, B.S., Strizhius, G.N., Brednev, V.I. et al. (1993) Hydrogen-induced brittleness and cold cracking in welding of steel 22Kh2NMFA. *Ibid.*, **8**, 3--10.
6. Kikuta, Y., Araki, T. (1980) Microscopic redistribution behaviours of hydrogen and fracture morphology of HAZ cold cracking in high strength steel. *IIW Doc. II-927--80*.
7. Brednev, V.I., Kasatkin, B.S. (1988) Specific work of cold cracking sites in welding of low-alloy high-strength steels. *Avtomatich. Svarka*, **11**, 3--8, 11.
8. Pokhodnya, I.K., Yavdoshchin, I.R., Paltsevich, A.P. et al. (2004) *Metallurgy of arc welding. Interaction of metal with gases*. Kiev: Naukova Dumka.
9. Boniszewski, T., Watkinson, F., Baker, R.G. et al. (1965) Hydrogen embrittlement and heat-affected zone cracking in low-carbon alloy steels with acicular microstructures. *British Welding J.*, 12(**1**), 20--42.
10. Kasatkin, B.S., Musiyachenko, V.F. (1970) *Low-alloy higher-strength steels for welded structures*. Kiev: Tekhnika.
11. Makara, A.M., Mosendz, N.A. (1971) *Welding of high-strength steels*. Kiev: Tekhnika.
12. Suzuki, H. (1978) Cold cracking and its prevention in steel welding. *IIW Doc. IX-1074--78*.
13. Terasaki, T., Hall, G.T., Parteger, R.I. (1991) Cooling time and prediction equation for estimating hydrogen diffusion in CTS test welds. *Transact. of JWS*, 22(**1**), 53--56.
14. Cottrell, A.H. (1944) A note on the initiation of hardened zone cracks. *Welding J.*, 23(**11**), 584--586.
15. Pidgaetsky, V.V. (1970) *Pores, inclusions and cracks in welds*. Kiev: Tekhnika.
16. Granjon, H. (1969) The «Implant» method for studying the weldability of high strength steels. *Metal Constr. and British Welding J.*, 1(**11**), 509--515.
17. Kasatkin, B.S., Brednev, V.I., Volkov, V.V. (1981) Procedure for determination of deformations in delayed fracture. *Avtomatich. Svarka*, **11**, 1--7, 11.
18. Belous, M.V., Braun, M.P. (1986) *Physics of metals*. Kiev: Vyshcha Shkola.
19. Krauss, G., Marder, A.R. (1971) The morphology of martensite in iron alloys. *Metallurgical Transact.*, 2(**9**), 2343--2357.
20. Kehoe, M., Kelly, P.M. (1970) The role of carbon in the strength of ferrous martensite. *Scripta Metallurgica*, 4(**6**), 473--476.

FEATURES OF RESISTANCE WELDING OF TITANIUM ALUMINIDES USING NANOLAYERED ALUMINIUM-TITANIUM FOILS

V.S. KUCHUK-YATSENKO, V.I. SHVETS, A.G. SAKHATSKY and A.A. NAKONECHNY
E.O. Paton Electric Welding Institute, NASU, Kiev, Ukraine

Peculiarities and prospects of application of resistance welding of titanium aluminides are considered. It is shown that nanolayer foils of the Ti--Al system used as inserts provide uniform heating of the workpiece and improve formation and properties of the joints.

Keywords: *resistance welding, titanium aluminide, nanostructured foil, microstructure, highly concentrated heating, heat-affected zone, near-weld zone*

Intermetallic alloys are capable of combining unique properties of metallic materials and chemical compounds, which is lately used in development of new structural materials, ensuring product performance under extreme conditions. The greatest number of works are devoted to development of intermetallic alloys based on titanium aluminide, which in the temperature range of 650--850 °C are superior to the applied high-temperature materials based on titanium, iron and nickel in terms of specific high-temperature resistance and specific modulus of elasticity, and are characterized by high high-temperature resistance and inflammability (Table). These alloys are effectively used as materials for gas turbine engine parts, flying

Properties of titanium aluminides

Intermetallic	E, GPa	δ_{20}, %	T_m, °C	ρ, g/cm^3	T_f, °C
Ti_3Al	141	2–5	1600	4.20	815
TiAl	180	1–2	1460	3.91	1040
Ti_2NbAl	130	3–5	–	6.90	800

vehicle skin, parts of load-carrying structure of aerospace products and other branches of engineering [1].

The main disadvantage of titanium aluminide is room temperature brittleness and the associated difficulties of its processing.

Future application of intermetallic alloys based on titanium aluminide is limited by absence of reliable methods of their joining to each other and other structural materials.

Diffusion welding in the temperature range of 1000--1100 °C with soaking for about 3 h under the pressure of 20--40 MPa enabled producing sound joints. Their strength characteristics, however, are greatly inferior to those of the base metal [2]. Joints produced by electron beam welding are prone to cracking which propagates from the fusion line [3].

At pressure welding [4] in a vacuum chamber at temperature of 750--850 °C the strength is extremely low because of line precipitates along the joint line. When aluminium foil is used as an interlayer, the weld develops defects in the form of microvoids and cracks, which also abruptly lower the strength. Titanium foil allows producing sound joints of a high strength. The weld, however, develops a layer of α_2(TiAl) phase, which does not meet the high-temperature strength requirements.

Unlike pressure welding, resistance welding provides a local high-speed application of heat and local deformation [5]. This welding process seems to be promising for joining high-temperature low-ductility materials, such as alloys based on titanium aluminides. Considering the experience of previous developments on resistance welding of aluminium alloys using nanolayered foils of Al–Cu and Al–Ni system as inserts [6], it was proposed to conduct welding of alloys based on titanium aluminides using nanolayered foils.

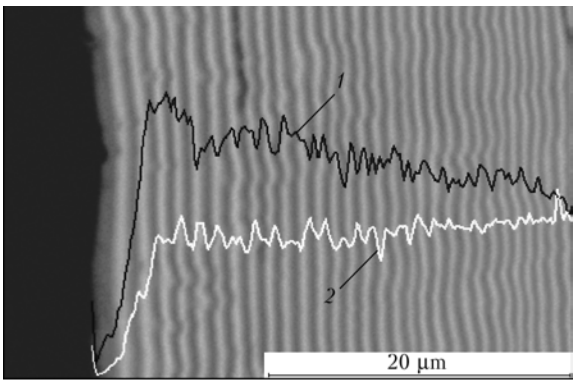

Figure 1. Microstructure (×2000) and microdistribution of titanium (*1*) and aluminium (*2*) in foil of Ti--Al system. Variations of Al and Ti content: 44.23--54.99 and 45.01--52.84 wt.%, respectively

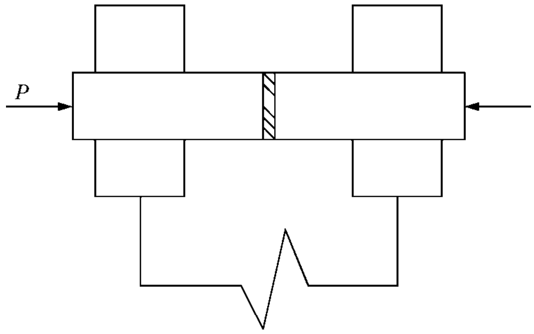

Figure 2. Schematic of resistance butt welding of Ti--47Al--1.5Cr--2Nb intermetallic alloy using foil (hatched part)

Nanostructured foils have been developed and are produced by PWI by EB PVD process. Foils used in this work were a multilayered aluminium-titanium combination, the average composition of which corresponds to the stoichiometric composition of γ-TiAl phase of Ti--Al system. Figure 1 gives the microstructure and distribution of titanium and aluminium in the foil. Heating of such a foil up to the temperature of approximately 300 °C leads to interaction of titanium with aluminium with formation of intermetallic [7]. The interaction reaction develops at a high speed and is accompanied by heat evolution: foil is heated up to «red heat».

Welding experiments were performed using Ti–47Al–1.5Cr--2Nb (at.%) alloy produced by electron beam melting at PWI.

Welding was conducted in a specialized butt welding machine K-766 (Figure 2). A feature of this unit consists in the absence of a common massive casing and a good balance of mobile column with the displacement force of 0.5–0.7 N. This ensures an effective operation of the pressure transfer mechanism, being particularly important at the resistance heating stage when using foils.

Metallographic investigations and analysis of chemical inhomogeneity of the joints were conducted in an optical microscope Neophot-32 and scanning electron microscope JSM-840 with Link-systems microanalyzer.

Strength properties of the joints were assessed by analysis of distribution of microhardness measured in LECO microhardness meter and by mechanical tensile tests.

Investigations were conducted on model samples of 15 × 15 × 110 mm size. Parameters of the welding mode selected in advance, were as follows: pressure at heating of 1.6–2.0 MPa, upset pressure of 40–45 MPa, welding time of 2.0–2.5 s. Both direct welding of the samples and welding through a 100 and 160 μm thick foil was performed.

First resistance welding of the intermetallic was conducted by the classical technology without using nanostructured foils. Investigation of the macrostructure of the produced welded joints showed the presence of micro- and macrocracks in the weld, metal of the HAZ and adjacent base metal (Figure 3, *b*). Ma-

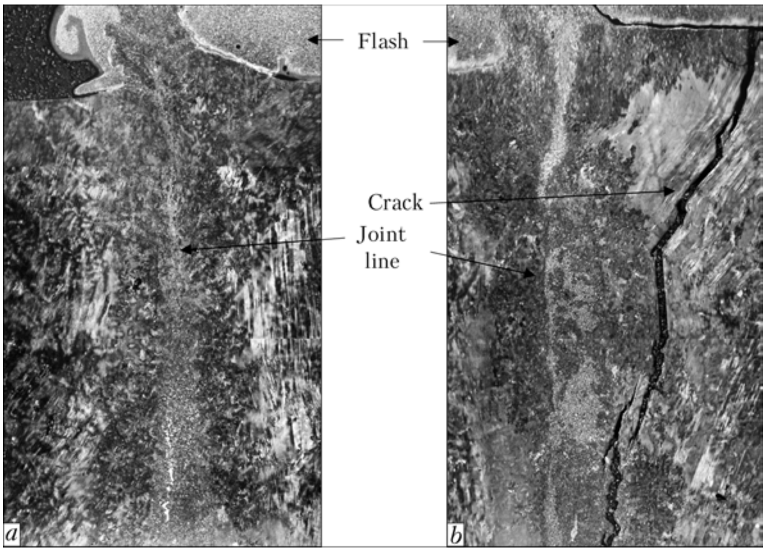

Figure 3. Macrostructure (×25) of joints of Ti--47Al--1.5Cr--2Nb intermetallic alloy made by resistance welding using foil of Ti--Al system (*a*) and without nanolayered foil (*b*)

chining of these welded joints when making the samples for mechanical testing led to their fracture.

Resistance welding using nanolayered foil is accompanied by intensive heat evolution in the contact zone, resulting in reduction of the welding time by 0.5–0.7 s on average, compared to regular welding. Better results were obtained using 60–100 μm foil.

Metallographic investigations showed that joints produced with application of foils have a stable macrostructure (Figure 3, *a*).

Visual control of samples (Figure 4) showed that in welding with foils the HAZ and amount of flash are reduced. Macrostructural analysis gives an idea about temperature distribution in welding. As is seen from Figure 5, use of foil ensures a more highly concentrated heating.

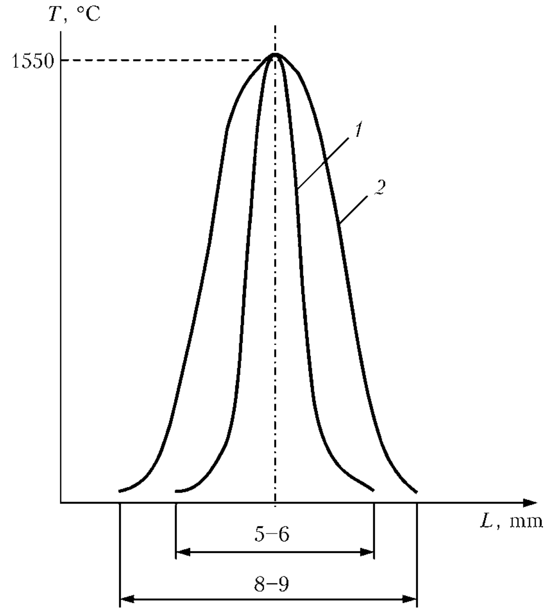

Figure 5. Temperature distribution in resistance butt welding of Ti--47Al--1.5Cr--2Nb intermetallic alloy with (*1*) and without (*2*) foil

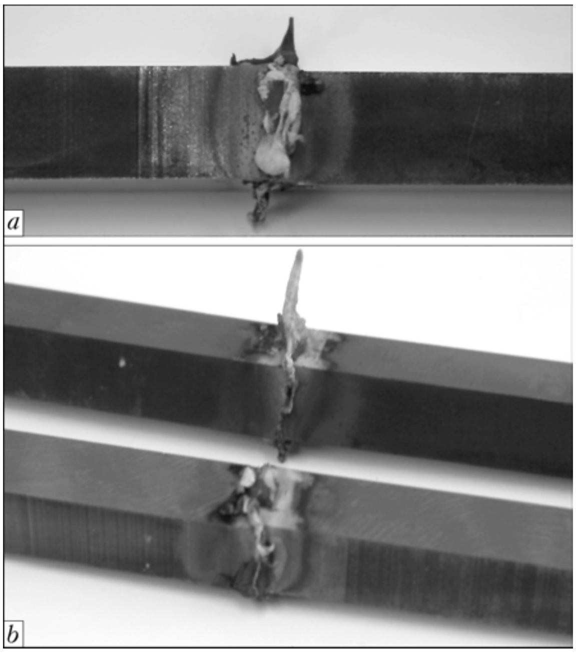

Figure 4. Samples of joints of intermetallic Ti--47Al--1.5Cr--2Nb alloy produced by resistance butt welding without foil (*a*) and using nanolayered foil of Ti--Al system (*b*)

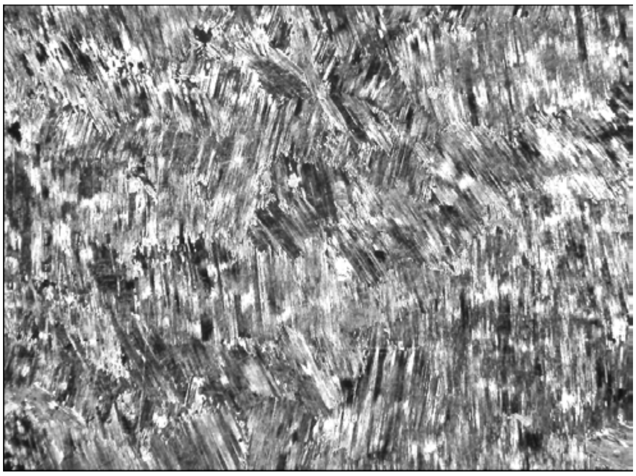

Figure 6. Microstructure (×100) of Ti--47Al--1.5Cr--2Nb intermetallic alloy

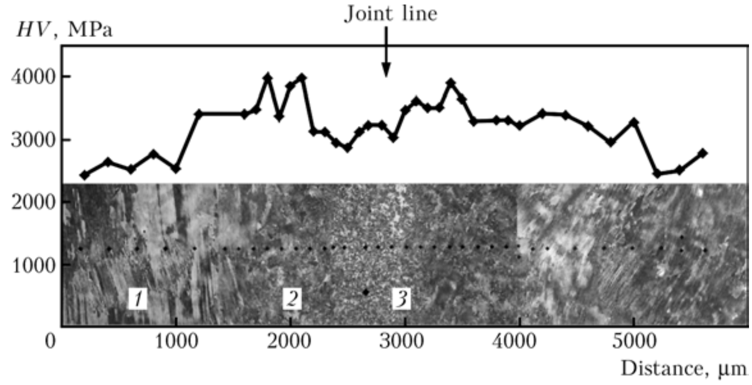

Figure 7. Microstructure (×100) and microhardness distribution (load of 4.9 N) in the metal of the joint of Ti--47Al--1.5Cr--2Nb intermetallic alloy made by resistance butt welding using foil of Ti--Al system: *1* ---- lamellar structure of base metal; *2* ---- refined lamellar structure; *3* ---- equiaxed grains of α-phase fringed by α_2-phase precipitates

Ti--47Al--1.5Cr--2Nb alloy has a predominantly lamellar structure, consisting of alternating plates of γ-TiAl and α_2-Ti_3Al phases (Figure 6). Globular grains of γ-phase of 100--150 μm size are also observed.

The welded joint produced using foil, is characterized by a clear-cut HAZ structure (see Figure 3, *a*). On the boundary with the base metal the lamellar structure becomes lighter (Figure 7, section *1*). This is, apparently, caused by partial dissolution of the dark-etching α_2-phase. This is followed by a layer of a refined lamellar structure (Figure 7, section *2*). A band of a refined equiaxed structure forms along the joint line: γ-phase grains fringed by α_2-phase (Figure 7, section *3*).

Products of the reaction of interaction in the foil were not detected optically. HAZ of the direct joint includes the same structural components; their location, however, is chaotic (see Figure 3, *b*). This is, obviously, related to temperature conditions of welding ---- non-uniformity of the temperature field along the joint. The arising thermal stresses can cause cracking in the HAZ metal.

Analysis of hardness distribution in the joint produced using foil (Figure 7) showed that in the section of a refined lamellar structure the microhardness rises compared to that of the intermetallic alloy from *HV*0.5-2500 MPa up to *HV*0.5-3500--4500 MPa. In the section with the refined equiaxed structure the hardness decreases and is equal to approximately *HV*0.5-3000 MPa.

Mechanical tensile testing of the joints was conducted on cylindrical samples MI-12 at room temperature. Rupture strength was equal to 295--310 MPa. Samples failed in the base metal.

When nanostructured foil of 160 μm thickness is used, the exothermal reaction is incomplete, so that the weld contains remains of the foil. Fracture of such welded joints at mechanical rupture testing occurs in the near-weld zone ($\sigma_{t\ max}$ = 270--280 MPa).

CONCLUSIONS

1. Resistance butt welding is characterized by local high-speed heat application and local deformation, respectively, which predetermines its attractiveness for producing joints of high-temperature materials with a low ductility (alloys based on titanium aluminide).

2. Use of nanolayered foils of Ti--Al system of 60--100 μm thickness as inserted elements in resistance butt welding improves the formation and properties of joints of alloys based on titanium aluminide owing to achievement of a uniform heating of the item.

3. When nanolayered Ti--Al foils of more than 150 μm thickness are used, more stringent welding modes should be applied.

1. Povarova, K.B., Bannykh, O.A. (2001) Structure and properties of alloys on the base of titanium aluminides. In: *Metals science and technology of light alloys*. Moscow: VILS.
2. Gam, G., Bohm, K.N., Kocak, M. (1999) Diffusionsschweissen fein gegossener Titanaluminide. *Schweissen und Schneiden*, **8**, 470--475.
3. Patterson, R.A., Martin, P.L., Damkroger, B.K. et al. (1990) Titanium aluminide: electron beam weldability. *Weld. Res. Supplement*, **1**, 39--44.
4. Yushtin, A.N., Zamkov, V.N., Sabokar, V.K. et al. (2001) Pressure welding of γ-TiAl intermetallic alloy. *The Paton Welding J.*, **1**, 33--37.
5. Kuchuk-Yatsenko, S.I. (1992) *Flash-butt welding*. Kiev: Naukova Dumka.
6. Kuchuk-Yatsenko, V.S., Shvets, V.I., Sakhatsky, A.G. et al. (2007) Specifics of resistance welding of aluminium alloys using nanostructured aluminium-nickel and aluminium-copper foils. *Svarochn. Proizvodstvo*, **9**, 12--14.
7. Ustinov, A.I., Olikhovskaya, L.A., Melnichenko, T.V. et al. (2008) Solid-phase reactions in heating of multilayer Al/Ti foils produced by electron beam deposition method. *Advances in Electrometallurgy*, **2**, 19--26.

ROLE OF PROTECTIVE COATING OF ALUMINIUM ALLOY WELDED JOINTS IN FATIGUE RESISTANCE

V.A. SHONIN, V.S. MASHIN, A.P. MURASHOV, V.I. ZELENIN, I.A. DEMIANOV, M.P. PASHULYA and **V.M. TEPLYUK**
E.O. Paton Electric Welding Institute, NASU, Kiev, Ukraine

Influence of thermal aluminium coating on mechanical properties of butt joints of AMg6 alloy with a longitudinal weld made by MIG welding and of the modulus of elasticity on the coating fatigue life was studied.

Keywords: *load-carrying structures, welded joints, aluminium alloys, protective coating, modulus of elasticity, fatigue resistance*

Under atmospheric conditions aluminium alloys are characterized by a high total corrosion resistance, however, with increase of their strength they are prone to point corrosion [1--3]. For load-carrying metal structures from wrought aluminium alloys of medium and high strength the main risk of accumulation of localized fatigue damage in the metal surface layers, particularly in the zones of stress raisers and welded joints, is presented by the environment and alternating loads in service [4--7]. Fatigue resistance of a structural element has maximum values in vacuum at minimum surface roughness [8], which is unachievable in real structures. Cladding by a layer of aluminium or its alloy with zinc of the thickness of 2--4 % of that of the base metal (BM) is used to protect the surface of rolled sheets from high-strength aluminium alloys from atmospheric impact [9]. A continuous protective layer features a lower fatigue resistance than that of BM and promotes a certain lowering of the clad metal fatigue life. In addition, in fusion welding an unprotected weld surface forms and protective coating in the near-weld zone is violated, which is one of the problems for efficient use of welding, particularly for high-strength clad alloys. Welded joint protection from atmospheric action is an important task and in this case the coating should not be the cause for or source of initiation of fatigue fracture of the joint.

For the conditions of simultaneous formation of the coating and the base, this problem can be solved, when the value of limit elastic deformation of the protective layer metal is higher than that of the welded joint metal. This condition can be expressed by the following inequality:

$$\frac{\sigma^p_{0.01}}{E^p} < \frac{\sigma^c_{0.01}}{E^c} \text{ or } \frac{\sigma^p_{R_\sigma,\,N}}{E^p} < \frac{\sigma^c_{R_\sigma,\,N}}{E^c}, \qquad (1)$$

where $\sigma_{0.01}$ is the conventional yield strength; $\sigma^p_{R_\sigma,\,N}$ is the fatigue limit for this value of the coefficient of cycle asymmetry R_σ and base fatigue life N; E is the modulus of elasticity, and indices p, c stand for the base and coating, respectively.

One of the ways to improve the metal coating deformability is lowering of the modulus of elasticity of the protective layer, which is achieved at increase of its discreteness with different methods of metal spraying [10--12].

The purpose of the work is substantiation of the prospects for application of protective coatings produced by spray-deposition of corrosion-resistant materials on welded joints of aluminium alloys operating under cyclic loads. In this connection the influence of protective thermal coating on the welded joint mechanical properties was studied in this work.

We studied fatigue resistance of welded joint of AMg6 alloy 2 mm thick with a longitudinal weld in as-welded condition and after application of aluminizing. Butt joint was made by MIG pulse welding in argon with SvAMg6 electrode of 1.2 mm diameter in the following mode: I_w = 90--95 A; U_a = 17.7--18.0 V; v_w = 50 m/h; $v_{w.f}$ = 335 m/min. Values of base current I_b (A) and pulse repetition rate F_p (Hz) were determined as $I_b = I_w/(1.5\text{--}2.0)$; $F_p = KI_b$, where K = 0.9--1.1. Welded joint coating of 0.17--0.26 mm thickness was applied with 2 mm wire of A5 aluminium using EM-14M arc metallizer at compressed air pressure of 6 atm in the following modes: I_a = 200--250 A; U_a = 36 V; spraying distance was 120 mm; consumed power of the process was 7.20--8.25 kW. The surface to be sprayed was prepared from two sides of the joint by liquid blasting by aluminium oxide chips of 14A grade with 80N grit (with grain size of 0.8--1.2 mm to GOST 3647--89, FePa standard, F16--F22 fraction). In this case compressed air was used at the pressure of 6 atm; distance to the surface was 60--70 mm; angle between the jet and treated surface was 75--90°. Roughness R_z = 15--20 μm was obtained.

Value of the modulus of elasticity was determined by indirect method by the results of tensile testing of BM samples with a two-sided coating and without coating. The refined values of the modulus of elasticity and mechanical properties of the coating were determined by direct tensile testing of coating samples which were made by peel spraying by aluminium. Spray-deposited metal samples of 120 × 10 × 3 mm size were cut out of blanks made by peel spraying on a copper substrate. The density of spray-deposited

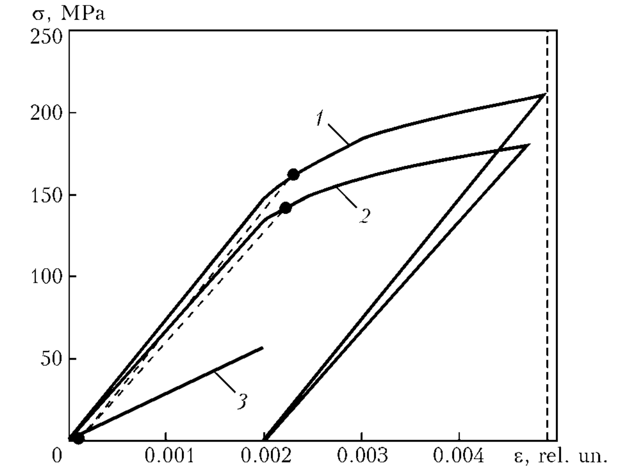

Figure 1. Experimental diagrams of deformation at tension up to the conventional yield point of samples of BM (*1*), coated BM (*2*) and calculated diagram of elastic deformation of the coating (*3*)

Table 1. Experimental values of the modulus of elasticity and elastic stresses for relative deformation $\varepsilon = 0.002$ of BM samples in the initial condition and with coating

Structural element	Element thickness t, mm	Stress $\sigma_{0.002}$, MPa	Modulus of elasticity E, GPa
BM	1.73	147.3	73.7
BM with an aluminium coating	2.03	133.9	66.96
Aluminium coating	0.3	56.6*	28.3*

*Calculated data.

metal of peel samples (2.22 g/cm^3) was determined by measurement of weight and volume. Tensile testing was performed using UME-10tm testing machine, strain gauge with 25 mm base and two-coordinate recorder N207/1.

At determination of the modulus of elasticity of the spray-deposited aluminium layer in coated samples it was assumed that residual stresses in the coating and base are minimum, and coating and base deformations are simultaneous, i.e.

$$\varepsilon = \frac{\sigma^p}{E^p} = \frac{\sigma^{pc}}{E^{pc}} = \frac{\sigma^c}{E^c}, \qquad (2)$$

where σ are the stresses in the structural element for a fixed value of relative deformation of the sample $\varepsilon = 0.002$; *pc* index is for base with coating.

Stresses σ^{pc} and σ^p were determined from deformation diagrams of coated and uncoated samples, and the value of stresses in the coating σ^c was calculated from load P^c, which develops in the coating for its concrete section F^c in the sample. At a fixed width of the structural elements the stress in the coating is expressed as

$$\sigma^c = \frac{P^c}{F^c} = \frac{P^{pc} - P^p}{F^c}, \qquad (3)$$

where P^{pc} and P^p are the experimentally established loads at testing of coated and uncoated samples for a fixed deformation and width of structural elements: $P^{pc} = \sigma^{pc}F^{pc}$ and $P^p = \sigma^p F^p$.

Diagrams of deformation at tension up to conventional yield point of coated and uncoated BM samples are given in Figure 1 together with the calculated diagram of elastic deformation of the coating, and values of the moduli of elasticity are given in Table 1. Nature of cyclic deformation of spray-deposited metal samples and fracture appearance are given in Figures 2 and 3, and mechanical properties are given in Table 2.

Results of determination of the coating modulus of elasticity on coated BM samples obtained by the standard procedure, agree well with the values of the modulus of elasticity, obtained by direct experimental testing on spray-deposited metal samples. Considering that the coating modulus of elasticity is almost 3 times smaller than the modulus of elasticity of the base, and at sufficiently high values of the yield and plastic limit of the spray-deposited metal it is anticipated that the coating at simultaneous deformation with the base, will not cause any premature fatigue damage of the welded joint.

Fatigue testing of butt joints with a longitudinal weld was conducted at zero asymmetry of cyclic tension in UE-10 machine. Load frequency was equal to 4–5 Hz. Separately welded flat samples of skeleton type of the overall dimensions of 250 × 60 × 2 mm with the working zone width of 30 mm and rounding-off radius of 140 mm were used. Weld width was equal to 7–8 mm. Three groups of welded samples were prepared for testing: as-welded; after preparatory operation of liquid blasting by aluminium oxide chips; with aluminium coating of the face and root surface of the joint.

Test results are presented by nominal stresses, which were calculated, proceeding from BM total cross-sectional area without allowing for aluminium

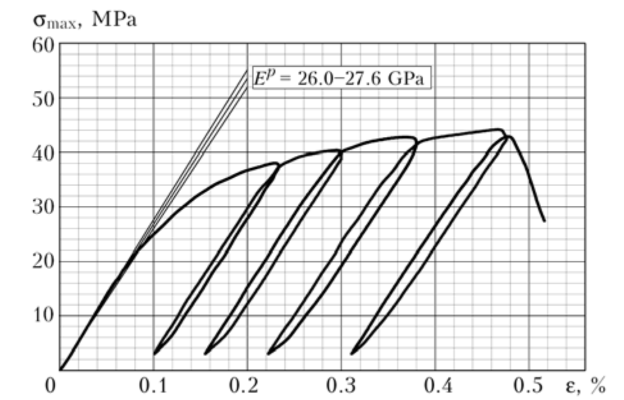

Figure 2. Diagram of deformation at cyclic tension to failure of a sample of peel spraying of aluminium

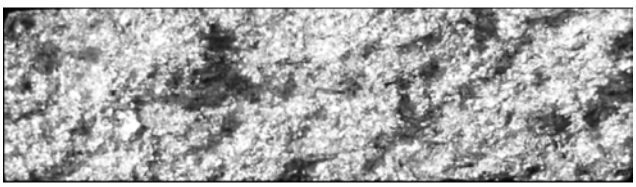

Figure 3. Appearance of fracture surface of a sample of aluminium peel spraying (×10)

Table 2. Experimentally determined mechanical properties of samples of AMg6 alloy BM in the initial condition and with aluminium coating, as well as samples of aluminium peel coating

Sample type	Sample section, mm^2	σ_t, MPa	$\sigma_{0.2}$, MPa	$\sigma_{0.001}$, MPa	δ_5, %
Uncoated BM	10 × 1.7	368.3	211.1	161.4	18.6
Coated BM (without allowing for coating thickness)	10 × 1.7	364.8	210.8	166.5	18.5
Coated BM	10 × 2	309.1	180.5	138.9	18.5
Peel spraying	10 × 3	44.2	42.0	24.4	0.3

coating in the sample working zone and by fatigue life to complete fracture of the welded joint (Figure 4). They are indicative of the fact that the coating does not influence the welded joint fatigue life. The data of fatigue resistance of coated welded joint samples are in the scatter band of the data obtained for as-welded joints. Also close to them are the results of testing samples after liquid blasting of the joint surfaces.

In the as-welded and coated samples cracks initiated in the weld metal, the main cause for which were defects, mainly individual fine pores, located in the upper or lower weld reinforcements. The layer of aluminium coating was not a source of crack initiation, and did not delaminate during fatigue crack propagation and final fracture of the cracked sample. Residual stresses which form as a result of liquid blasting and subsequent aluminizing, are not involved in fatigue damage of the welded joint. It is obvious that their levels in the surface layers are not high enough, as presence of residual stresses could have a noticeable influence on the change of the modulus of elasticity of the base, which is confirmed by comparison of mechanical properties of BM samples in as-welded and coated condition (see Table 2). Here the sprayed metal layer as a design element takes up a small part of the load.

Thus, in order to ensure the resistance of the protective coating against premature fatigue damage during long-term operation of the structural element with a welded joint, a low value of the modulus of elasticity of the coating compared to the base is an important characteristic. Coating reliability under the conditions of simultaneous deformation with the base is also provided by sufficient ductility of the spray-deposited metal, which promotes compensation of higher elastic deformations of the base.

In conclusion, it should be noted that corrosion protection measures cannot be the cause for lowering of the base fatigue resistance, if the modulus of elasticity of the spray-deposited protective coating is lower than that of the base.

Value of the coating modulus of elasticity should be determined by calculation from the stress--strain diagrams, obtained at comparative tensile testing of coated and uncoated BM samples. It is shown that these data agree with direct measurements of the modulus of elasticity on samples of peel spraying of a protective alloy.

It is established that application of electric arc metallization by corrosion-resistant aluminium A5 for welded joints of AMg6 alloy with a longitudinal weld made by MIG pulse welding, does not lower the fatigue resistance of the base under the conditions of an axial alternating load with zero-to-tension cycle. Technology of thermal spraying by aluminium can be recommended as a protective coating for welded joints of high-strength aluminium alloys under the condition, provided the coating is characterized by a greater deformability than the base.

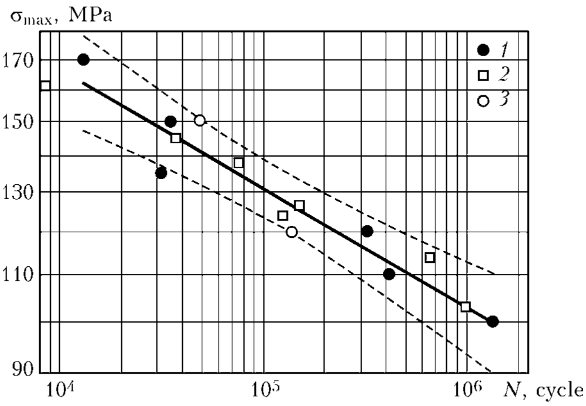

Figure 4. Fatigue resistance at zero-to-tension axial cyclic load of butt joints of AMg6 alloy with a longitudinal weld made by a consumable electrode (MIG pulse method): *1* ---- initial condition; *2* ---- after abrasive cleaning; *3* ---- with a protective aluminium coating layer applied by electric arc spraying

1. Abolikhina, E.V., Molyar, A.G. (2003) Corrosion of aluminium alloy structures. *Fiz.-Khimich. Mekhanika Materialov*, **6**, 106--110.
2. (1972) *Aluminium alloys. Commercial deformable, sintered and cast aluminium alloys*: Refer. Book. Ed. by F.I. Kvasov, I.N. Fridlyander. Moscow: Metallurgiya.
3. (1971) *Aluminium-handbuch*. Berlin: VEB Verl. Technik.
4. (1972) *Aluminium alloys. Application of aluminium alloys*: Refer. Book. Ed. by A.T. Tumanov. Moscow: Metallurgiya.
5. Karlashov, A.V., Gnatyuk, A.D., Kardash, A.B. (1982) Corrosion-fatigue strength of aluminium alloys. In: *Proc. of 1st Sov.-Engl. Seminar on Corrosion Fatigue of Metals*. Kiev: Naukova Dumka, 206--229.
6. Kushnarenko, V.M. (1973) *Resistance of AMg6 alloy welded joints under stress corrosion*: Syn. of Thesis for Cand. of Techn. Sci. Degree. Moscow: N.E. Bauman MVTU.
7. Zverev, A.I., Kopetman, L.N. (1990) Influence of detonation coatings on fatigue resistance of parts. *Poroshk. Metallurgiya*, **5**, 37--41.
8. Nejman, P. (1987) *Physical metals science*. Vol. 3. Moscow: Metallurgiya.
9. (1974) *Aluminium alloys. Structure and properties of semi-finished products from aluminium alloys*: Refer. Book. Ed. by V.A. Livanov. Moscow: Metallurgiya.
10. Lyashenko, B.A., Kuriat, R.I. (2005) Coatings and their application in engineering. In: *Strength of materials and structures*. Kiev: Akademperiodika.
11. Dolgov, N.A. (2002) Influence of elastic modulus on serviceability of substrate--coating system. *Problemy Prochnosti*, **2**, 66--72.
12. Hasui, A., Morigaki, O. (1985) *Surfacing and spraying*. Ed. by V.S. Stepin, N.G. Shesterkin. Moscow: Mashinostroenie.

EXPERIENCE IN DESIGNING AND MANUFACTURE OF WELDING-AND-SURFACING INSTALATIONS

V.I. TITARENKO[1], O.V. TKACHENKO[1], D.Yu. MATIKO[2], V.I. PILIPKO[2],
I.F. MUDRANINETS[2] and I.I. MUDRANINETS[2]
[1]«NPP REMMASH Ltd.», Dnepropetrovsk, Ukraine
[2]OJSC «Ilnitsk Zavod MSO», Ilnitsa, Ukraine

The experience in work of a small enterprise in design and manufacture of specialized welding-and-surfacing equipment using modular principle and wide cooperation has been considered. The system works of some installations and fields of their application are described.

Keywords: *arc surfacing, surfacing installations, modular design, cooperation, specialization*

In accordance with the market demands in the branch of welding and surfacing machine-tools and installations over the recent ten years NPP REMMASH Ltd has gained the experience in design and manufacture of such kind of equipment. This approach includes the following basic elements:

- comprehensive analysis of analogues of equipment developed;
- application of a modular design principle featuring that general design of certain installation depending on the engineering task consists of single modules (blocks) designed before. It allows the efficient offer of equipment sketch to a customer corresponding to the technical assignment and its further timely realisation into a ready-made structure;
- maximum attraction of co-designers and co-manufacturers, developing and manufacturing the separate ready-made units for equipment that enables reduction of manufacturing terms as much as possible retaining the high quality of separate units manufactured by the enterprises specialised on the development and production of these units and as a result of the equipment as a whole;
- imparting the functions of versatility to any special installation, thus increasing the load and output capacity of installations;

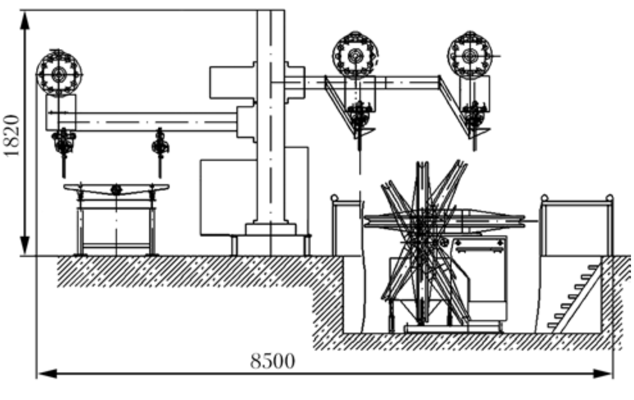

Figure 1. Schematic diagram of installation of RM-15 type

- maximum possible equipping of each installation with technological outfit which allows improving the quality, stability, efficiency and safety during operation;
- customization of each installation on the basis of pre-developed typical installations, that does not need adaptation of an installation to customers requirements but allows immediate putting into operation, thus minimizing time of implementation.

Considering the aforesaid and expanding the nomenclature of developed welding and surfacing machine-tools machines and installations, REMMASH in cooperation with OJSC «Ilnitsky Zavod MSO» and a number of other enterprises has manufactured some new types of equipment. Among this equipment there are installations for surfacing of large-sized parts (RM-15 type for deposition of rope blocks of diameter up to 2.5 m), as well as machine-tools for welding-and-surfacing of small-sized parts (RM-165 and IZRM-5 types).

The RM-15 installation for surfacing of rope blocks was developed and manufactured on order of OJSC OGOK. The installation, already existing at the customer facility, was taken as an analogue. It had some critical structural disadvantages which in general did not impede the realisation of surfacing technology at the blocks restoration, but complicated its realization by the negative influencing the efficiency and surfacing quality. Therefore, the specialists of OGOK together with REMMASH have developed the technical assignment for the radically new design of installation, which was realised by REMMASH together with «Ilnitsky Zavod MSO» into the installation RM-15 (Figure 1).

By its conception and design, it is notably distinguished from the previous one operating at the OGOK. The only similar to the previous design part of installation RM-15 is the versatile rotator located in a pit. At the same time, taking into account that general design of equipment in contrast to the analogue provides all setting-up and technological operations even without a rotator, it stands fixed on the separated lugs to increase stability, reliability and safety in the operation of the rotator when different overloads are possible.

The surfacing automatic machine is mounted on the site of a mobile console of a stationary turn pillar installed and fixed on the basement bolts. The mobile console on which the surfacing automatic machine is mounted has longitudinal, horizontal working technological and travel movement of 1800 mm and vertical adjusting travel movement of 1600 mm. As the technological working movement of the console with automatic machine is transverse in surfacing of rope blocks with respect to circular beads being deposited in movement per a pitch of deposition, the electric diagram of the installation provides the automatic transition of the automatic machine (if required) after each full revolution per a pre-selected pitch from 1 to 20 mm.

The vertical movement of console in combination with the vertical movement of the surfacing automatic machine, provides the total vertical movement of 2100 mm, thus enabling surfacing not only of all surfaces of all types and sizes of rope blocks, but also expanding the technological capabilities of the installation and possible nomenclature of parts which can be surfaced. For example, it allows including the surfacing of inner surfaces of cylindrical parts of up to 600 mm and even up to 1000 mm on the prolonged nozzle into nomenclature of parts surfaced in the installation, moreover, that such parts, requiring restoration are available at OGOK.

The automatic machine A-1406 arc supply with welding current is performed from the welding rectifier KIU-1201 included into the set of installation RM-15, and electric diagram control of installation is performed from its control panel through the control cabinet. Both the rectifier and the control cabinet are mounted on a special platform of a stationary turn pillar, rotating together with its turn.

To collect the used flux which is poured together with the slag during rotation from the block being deposited, the installation is furnished with a special device, manufactured in the form of a hopper on the telescopic lugs, a sieve of 5 mm cell is mounted on upper its plane and ejector — in the lower part. The sieve allows screening the used mixture of flux with a slag, falling from rotating parts being surfaced, dividing this mixture into slag, which is remained on the sieve mesh and periodically removed, and screened flux, poured into a hopper and reused. Ejector, to which the compressed air of pressure 3–5 atm is supplied, transports the air-flux mixture upwards to the flux hopper of the surfacing automatic machine for reuse. The hopper telescopic lugs are mounted for a required height that along with horizontal movement allows the selection of its optimal spatial location for each type and size of surfacing block and collection of the main part of flux-slag mixture pouring from the block being surfaced.

Taking into consideration the big variety of types and sizes of the parts restored at the OGOK, including those of non-cylindrical shape, there was a need in design and manufacture of the installation to provide its maximum versatility. In order to realise this for the RM-15 istallation, a table for surfacing of plane parts was designed, and then manufactured and included into the set. Taking into consideration that surfacing automatic machine is mounted on the turn pillar for transition from surfacing of rope blocks and other cylindrical parts to surfacing of plane parts, mounted on the table, it is required only to turn over the pillar that takes several seconds. Here, the table is fixed in any suitable place within the working area of surfacing automatic machine considering the possibilities of the pillar turn with a console on which it is fixed and turned by the angle 360°. The table is fixed in a way that the horizontal movement of the console with the automatic machine could provide the surfacing of longitudinal beads of parts fixed on the table, and the transverse movement per a pitch of surfacing is provided by a screw mechanism of the table itself.

The installation RM-15 demonstrated the significant advantages in contrast to the previous installation of a gantry type, which are featured both by a convenience of service and also by the quality surfacing, namely: the operation of mounting and fixturing the part being surfaced on the faceplate of rotator was simplified, which is facilitated by the location of surfacing automatic machine on the turn pillar, that in its turn allows free withdrawal from the working area during the mounting of the block. The range of longitudinal horizontal movement of console with the surfacing automatic machine within 1800 mm enables surfacing of all types and sizes of blocks in all technological positions without the additional re-arrangement of the rotator as it was used in the old installation. The possibility of automatic movement per a required pitch of surfacing enables more accurate surfacing of necessary configuration of a worn-out surface, considerably reducing the consumption of surfacing materials, labour intensity and subsequent mechanical treatment. In combination with the big potential of expansion of nomenclature of parts, being surfaced in the installation, due to the surfacing of plane parts and inner surfaces of cylindrical parts, this testifies to the successful variant of designing solution and completing in the manufacturing of installation RM-15.

Besides the large-size parts, for the surfacing and welding of which the installations RM UN-5, RM-10, RM-15 and others can be used, there is a wide nomenclature of small-sized parts, for welding-deposition of which REMMASH together with «Ilnitsky Zavod MSO» developed two types of installations: RM-165 and IZRM-5.

The installation RM-165 (Figure 2) has been developed and manufactured on the order of OJSC DMKD for completing the complex KAS RM-165 designed for restoration of agglomeration workshop rollers. The basic variant of this installation allows the deposition by a self-shielding flux-cored wire of the outer and inner surface of rollers of diameter up to 300 mm, length up to 500 mm and weight up to 63 kg.

The installation consists of a table-basement *1*, on which a versatile welding rotator *2* and turn pillar *3*

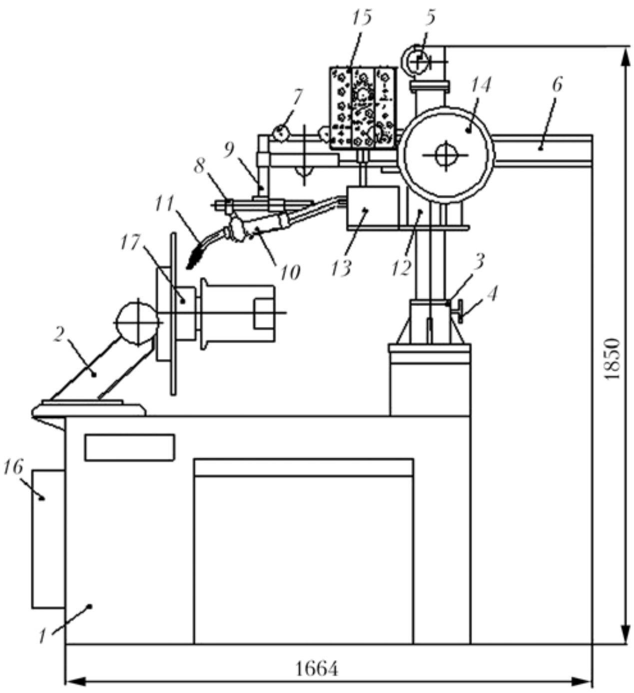

Figure 2. Schematic diagram of installation of RM-165 type (for designations see the text)

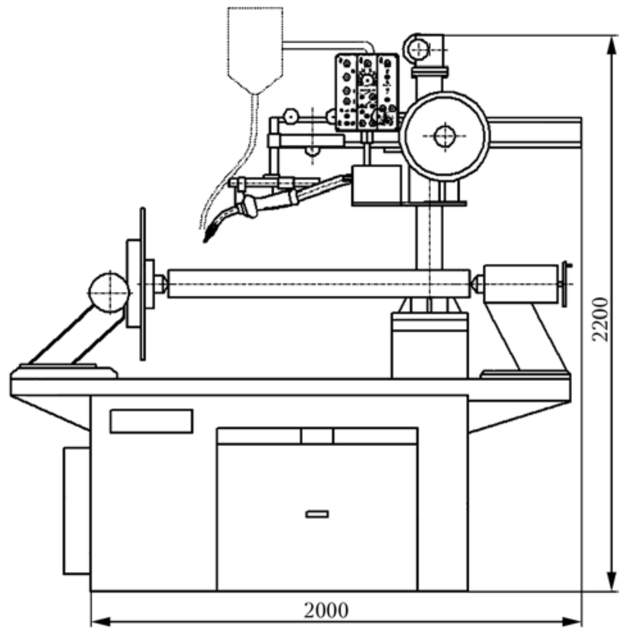

Figure 3. Schematic diagram of installation of IZRM-5 type

are fixed. The pillar, turning into setting and working position, has a fastener of necessary position *4* and a drive *5* for vertical movement of traverse *6*, on which the automatic machine is mounted and moved. The latter is mounted on two carriages: driven *7* and non-driven *12* connected with it, on which a feeding mechanism *13* and spool holder *14* for a spool with a welding-surfacing wire are mounted. On the driven carriage *7* devices *8* and *9* are mounted for nozzle correction relative to the part being surfaced, in which the nozzle body *10* and its guide *11*, feeding wire to the zone of welding, are fixed. The rollers being welded and surfaced are fixed in a special fixture *17* mounted on a rotator faceplate *2*. The installation control is performed from the control panel *15* using electrical diagram wired in the control cabinet *16* positioned in the installation table-basement *1*. The installation is completed with a versatile welding rectifier mounted next to the table-basement.

In designing and manufacturing the complex KAS RM-165 a modular principle with a wide cooperation with enterprises-manufacturers of completing units and welding-surfacing equipment was applied. Moreover, not only the serially-manufactured parts with their further modification and adaptation to the installation were purchased in these enterprises, but the parts were also ordered and manufactured by the special technical orders of basic developers of the equipment. For this work, OJSC SiMZ, supplying the completed feeding mechanism and power source, OJSC «Artyom Kontakt», supplying by a special order the mechanism of welding tractor movement were attracted. «Ilnitsky Zavod MSO» played a special role in the development of installation and complex having not only manufactured several basic units according to the technical assignment at once: body, rotator, pillar, but also participated in designing and manufacture of the whole installation. Such an approach and organization of manufacture allowed the development and manufacture of installation RM-165 and the complex as a whole in three months. The additional positive moment of development and manufacture of the installation is its perspective in creation of the whole range of small-sized machine-tools and installations for other kinds of arc welding-surfacing, such as electric submerged arc and shielded-gas arc method and also for another groups of parts like shaft and plate.

More versatile machine-tool was developed and manufactured by REMMASH in collaboration with «Ilnitsky Zavod MSO». This is a versatile machine-tool IZRM-5, designed for automatic arc welding-surfacing under fluxes, in shielding gases and using self-shielding flux-cored wire of cylindrical parts of diameter up to 400 mm, length up to 1000 mm and weight up to 120 kg.

Unlike the installation RM-165, the installation IZRM-5 (Figure 3) is additionally equipped with a rear post, hopper for flux and hopper for collection of slag and used flux. Moreover, the installation IZRM-5 set includes additionally nozzles-torches for welding-surfacing in shielding gases and under flux, and also a gas control equipment.

The described approaches towards the designing and manufacturing, realized in a close cooperation with the customers of welding-surfacing equipment allowed NPP REMMASH Ltd together with OJSC «Ilnitsky Zavod MSO» to design and manufacture over the recent several years the whole series of installations both by purpose and also by dimensions of parts, being welded and surfaced, covering their wide nomenclature.

EFFICIENCY OF STABILISATION OF THE ALTERNATING-CURRENT ARC IN COVERED-ELECTRODE WELDING

A.F. SHATAN, A.A. ANDRIANOV, V.N. SIDORETS and **A.M. ZHERNOSEKOV**
E.O. Paton Electric Welding Institute, NASU, Kiev, Ukraine

Efficiency of the optimised modes for stabilisation of the alternating-current arc was studied. It is shown that manual a-c arc welding of 18-10 type steel provides properties of the welded joints similar to those achieved with d-c welding.

Keywords: *corrosion-resistant steel, arc welding, alternating welding current, arc stabilisers, microstructure, corrosion*

Despite the success achieved in the last decades in the field of development and commercial application of welding arc power supplies (inverters, digital control systems with regulation of the welding current waveform), welding with the commercial-frequency alternating-current arc is still extensively used and currently important [1, 2]. Studies of this welding method stand in importance with current studies of CO_2 welding, which provides sound welded joints despite a wide use of multi-component gas mixtures.

Utilisation of arc stabilisers in a-c welding allows decreasing the open-circuit voltage of a transformer and consumption of electrotechnical materials [1, 3]. So far, there is no agreement regarding parameters of a stabilising pulse, such as energy of the pulse, time of its feeding (injecting) relative to the time of transition of the welding current through zero, and its polarity. The authors of study [4] managed to formulate and solve this problem. The optimisation criterion in that case was a minimal open-circuit voltage of a power supply at which the arc is still burning, and the variable parameter was a difference of phases between the welding current and stabilising pulse. The a-c welding arc was described by using the generalised mathematical model of the dynamic arc developed by the E.O. Paton Electric Welding Institute.

Study [4] determined dependence of the minimal open-circuit voltage of a welding transformer, at which the arc is burning, upon the difference of phases between the welding current and stabilising pulse (Figure 1). As follows from the plotted curves, dependence of the voltage has clearly defined minima. This means that the optimisation problem is solvable. Moreover, it proves the fact that utilisation of the stabilising pulses, the polarity of which is opposite to that of the arc current, is more preferable, as in this case the curve of minimal open-circuit voltage $U_{\text{o.-c min}}$ is lower than in the case of using pulses with a positive polarity. Study [4] gives explanation to this fact: the stabilising pulse directed opposite to the welding current does not hamper operation of the main power supply and favours the situation where, after the end of the stabilising pulse, the main power supply operates as a stabilising device.

The purpose of this study was to experimentally investigate the efficiency of stabilisation of the a-c arc in manual arc welding of corrosion-resistant steels.

Manual a-c welding was performed by using the welding transformer with a decreased open-circuit voltage and optimised arc stabiliser (OAS). To compare, a-c cladding and welding were performed by using a rectifier of the VD-306 type. The investigations were conducted on corrosion-resistant steel 12Kh18N10T, 4 mm thick, by using 3 mm diameter electrodes of the OZL-8 grade. Reportedly [5], the electrodes of this grade are intended for welding at a direct current of reverse polarity. Beads were deposited on plate of the above steel to check stability of the arc burning at the alternating current. Utilisation of OAS allows the welding process to be performed at the alternating arc without extinction of the arc and with minimal spattering.

To investigate the quality of metal of the welded joints, a highly skilled welding operator performed welding of the square-groove butt joints in one pass with a gap of 1.5 mm at the direct current (sample 1, mean value of welding current I_{mean} = 85–90 A), and at the alternating current with OCS (sample 2, effec-

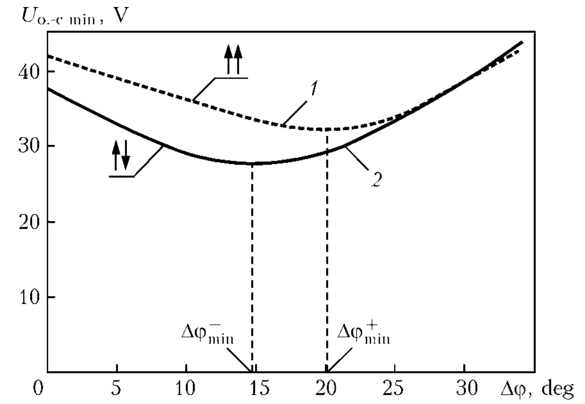

Figure 1. Dependence of minimal open-circuit voltage of welding transformer, at which the arc is burning, upon the difference in phases between the welding current and stabilising pulse: *1* –– polarity of the stabilising pulse coincides with polarity of the welding current; *2* –– opposite polarity

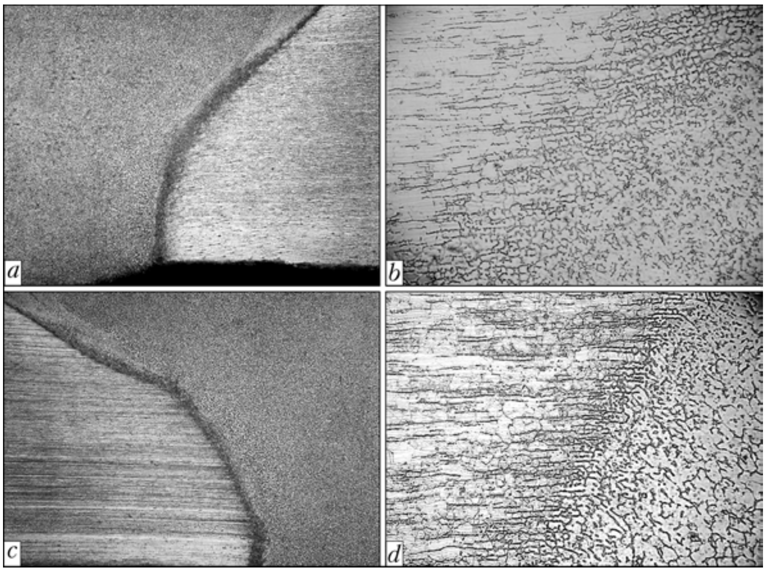

Figure 2. Macro- (*a, c* ---- ×25, reduced 3.5 times) and microstructure (*b, d* ---- ×200, reduced 3.5 times) of regions of the welded joints produced at the direct (*a, b*) and alternating current by using OCS (*c, d*)

tive value of welding current I_{eff} = 95–97 A). The weld metal had the following chemical composition, wt.%: sample 1 ---- 0.082 C, 0.75 Si, 1.0 Mn, 18.6 Cr, 9.5 Ni, 0.20 Ti, 0.3 Cu; and sample 2 ---- 0.082 C, 0.75 Si, 1.0 Mn, 18.9 Cr, 9.6 Ni, 0.19 Ti, 0.3 Cu.

Metallographic examinations of the welded joints were carried out by using the «Neophot-32» microscope at different magnifications. Digital images of the microstructures were obtained by using the «Olympus» photographic camera. The presence of δ-ferrite was detected with the «Ferritgehaltmesser-1053» ferrite meter.

Samples 1 and 2 had an almost identical structure of the weld metal, which consisted of cast austenite with a small amount of δ-ferrite (1.5–2.5 vol.% in sample 1, and 1.5–1.7 vol.% in sample 2). Carbonitrides (yellow-pink inclusions of a regular geometric shape) were revealed in metal of both welds.

No cracks or other defects were detected along the fusion line and in HAZ. The HAZ metal of both samples was characterised by an austenitic structure with δ-ferrite precipitating along the rolling direction in the form of thin interlayers (Figure 2). Austenite grains in a coarse-grained region of the HAZ metal of samples 1 and 2 had a size of 5–6 (according to GOST 5639--82). Metal of a fine-grained region of these samples had a granular austenitic structure (grain size ---- 7–8) with δ-ferrite precipitating along the rolling direction. The base metal of samples 1 and 2 had an identical, fine-grained austenitic structure with a grain size of 10--11 (according to GOST 5639--82), comprising thin interlayers of δ-ferrite precipitating along the rolling direction, as well as carbonitrides (Figure 2).

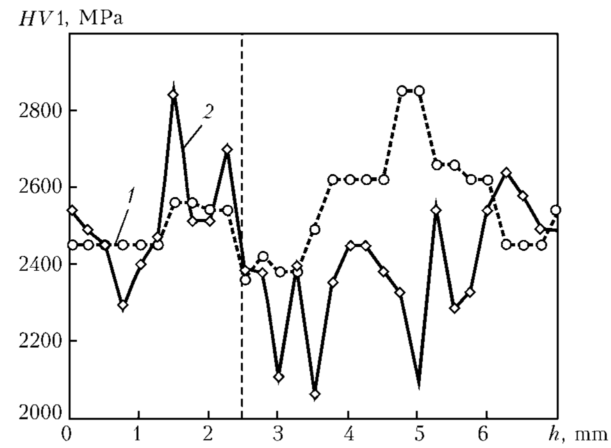

Figure 3. Distribution of microhardness in welded joint produced at the direct (*1*) and alternating current by using OCS (*2*): dashed line ---- fusion line; *h* ---- distance from the weld centre

Microhardness was measured by using the LECO microhardness meter M-400. Figure 3 show the results of measuring microhardness of the welded joints (from the weld centre) with a step of 0.25 mm. As seen from Figure 3, the changes in values of microhardness of a welded joint produced at the alternating current with OCS are more substantial, compared with the case of using the direct current. However, they do not exceed the tolerable limits in welding with the said grade of electrodes.

The Table gives results of mechanical tests of specimens of the butt welded joints conducted at a temperature of 20 °C (three specimens for each type of the tests). It can be seen from the Table that tensile strength σ_t of the welded joint on steel 12Kh18N10T produced at the direct current is a bit higher, and impact toughness *KCV* is lower than in the case of using the alternating current and OCS.

In addition, 20 × 80 mm specimens cut out from the butt joint with a removed reinforcement were investigated to study resistance to pitting corrosion in

Mechanical properties of butt welded joints

Welding current	σ_t, MPa	*KCV*, J/cm^2
Direct	$\frac{603.3–651.1}{634.3}$	$\frac{96.8–124.1}{107.0}$
Alternating with OCS	$\frac{594.5–600.1}{595.8}$	$\frac{95.8–126.5}{112.4}$

10 % $FeCl\cdot6H_2O$ solution at 20 °C (GOST 9.912--89). It can be concluded from values of the conditional pitting corrosion rate that the specimens tested had little difference from the welded joints produced at the direct current using electrodes OZL-8.

Therefore, the mathematical model of the welding arc developed by the E.O. Paton Electric Welding Institute allows optimisation of parameters of the stabilising pulse used in a-c welding, based on the electrotechnical and weight-size criteria. Utilisation of the optimised modes of stabilisation of the arc in manual arc welding of corrosion-resistant steels at the alternating current provides welded joints with the same high quality indicators as in welding at the direct current. The positive solution of the optimisation problem for manual arc welding makes the application of such approaches promising for optimisation of other welding processes as well.

1. Paton, B.E., Zaruba, I.I., Dymenko, V.V. et al. (2006) Lowering of material content of power sources and power consumption in welding. *The Paton Welding J.*, **10**, 15--23.
2. Kiji, N., Kobayashi, K., Ishii, J. et al. (2003) Development of high efficiency arc welding methods. *Ibid.*, **10**, 56--60.
3. Zaruba, I.I., Dymenko, V.V., Bolotko, V.I. (1989) Welding transformers with arc stabilization devices. *Avtomatich. Svarka*, **10**, 46--51.
4. Andrianov, A.A., Sidorets, V.N. (2009) Optimisation of parameters of a-c welding arc stabilization. *Elektrotekhnika i Elektromekhanika*, **2**, 5--12.
5. (1994) *Consumables for welding of steels and cast iron*: Refer. Book. Ed. by V.N. Gorpenyuk. Kiev: Hauch. Kniga.

WELDING REPAIR OF SURFACE DEFECTS IN Ml-10 ALLOY CASTINGS BY USING SCANDIUM-CONTAINING MATERIAL

V.A. SHALOMEEV[1], **E.I. TSIVIRKO**[1], **I.A. PETRIK**[2] and **V.V. LUKINOV**[2]

[1]Zaporozhie National Technical University, Zaporozhie, Ukraine

[2]OJSC «Motor-Sich», Zaporozhie, Ukraine

The effect of scandium content in filler alloy Ml-10 on quality of welding-repaired cast magnesium parts has been studied. It is noted that scandium exerts a modifying effect on mechanical properties and heat resistance of the alloy. Utilisation of the scandium-containing filler metal for welding repair of alloy Ml-10 parts leads to a substantial increase in the level of mechanical properties of weld metal.

Keyword: *TIG welding, alloy Ml-10, filler material, welding repair of defects, scandium, modifying*

Aircraft engines, being in operation for a specified time, are subjected to maintenance inspections to increase their reliability and extend their service life, in the course of which surface defects are detected on their individual elements and then repaired by welding [1].

Ml-10 alloy is widely applied for production of heat-resistant magnesium castings for aircraft engine engineering. The alloy contains zirconium and neodymium, which provide the required operating characteristics of the alloy at elevated temperatures by forming heat-resistant intermetallic phases [2]. The range of cast parts manufactured from alloy Ml-10 is very diverse, and the cost of complex casing parts may amount to dozens of thousands of UAH. Therefore, special attention is given to the technological issues associated with their repair.

After operation, small cracks (Figure 1) form as a rule on the surface of parts of alloy Ml-10, which is caused by service conditions of the aircraft engines. Cracks of a mixed type are most common, the fatigue-corrosion cracks being dominant. Surface of the opened cracks has a heterogeneous structure, it is cov-

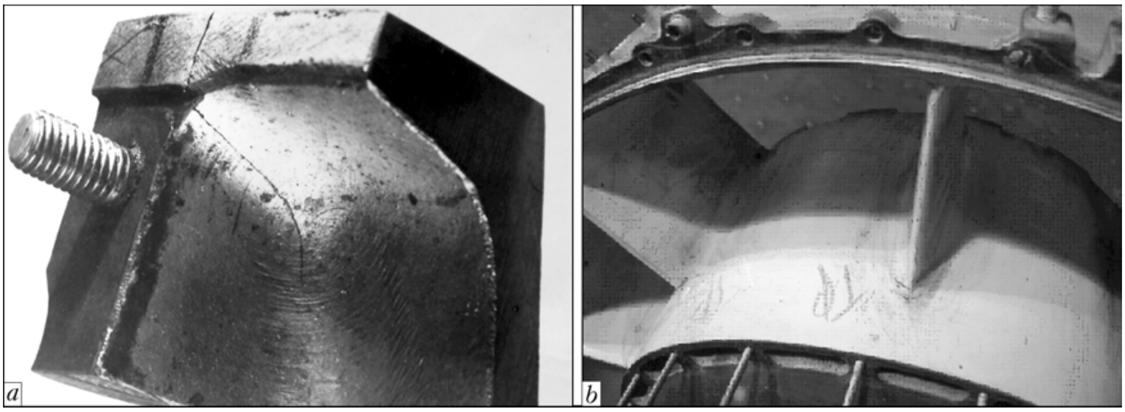

Figure 1. Appearance of cracks on the surface of Ml-10 alloy castings: *a* ---- fragment of front casing; *b* ---- casing part

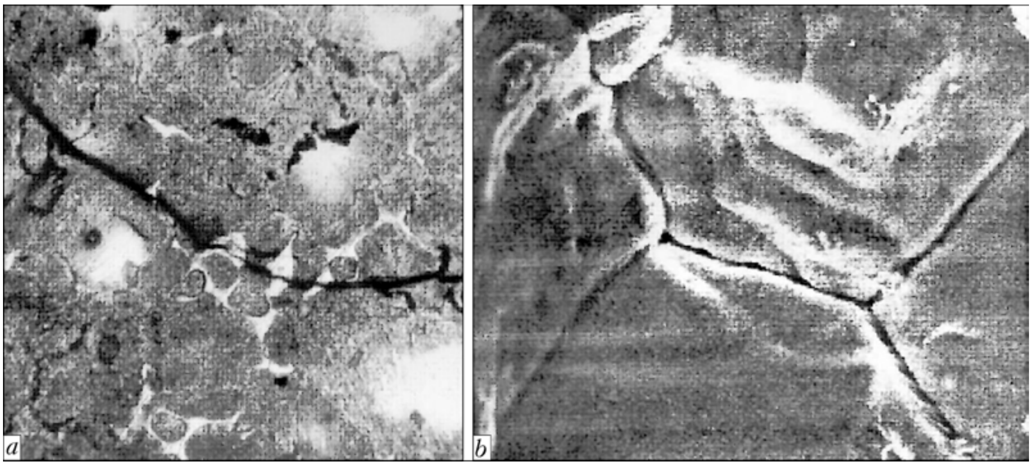

Figure 2. Microstrucure (×210) of magnesium alloy with crack (*a*) and partial melting of grain boundaries (*b*)

ered by a thick layer of oxides. A crack may propagate through grain as well as along its boundaries (Figure 2, *a*).

Microscopic analysis showed that partial melting of grain boundaries (Figure 2, *b*) and intergranular failure, which is characteristic of the overheated state, take place in a coarse-crystalline structure of the alloy.

According to specifications, after detection and machining of a defect, it is permitted to employ tungsten-electrode argon-arc welding using a filler metal of alloy Ml-10 to repair this defect. There were cases when new cracks formed in welding repair of defects, which led, in separate cases, to rejection of parts. In this connection, development of new filler metals for welding repair of defects in cast parts is very important for ensuring their required quality.

It is well known that scandium has a positive influence on welded aluminium alloys [3] and aluminium-containing alloys [4, 5] due to the formation of heat-resistant intermetallic phases. Therefore, it is of interest to investigate the effect of scandium on structure and properties of heat-resistant alloy Ml-10 containing heat-resistant phases $(MgZr)_{12}Nd$, the presence of which promotes increase of physical-chemical characteristics in the welding repair location.

Investigations were carried out in two stages:

• development of scandium-containing filler alloy Ml-10 with an optimum content of scandium to provide improved mechanical properties and heat resistance;

• study of structure and properties of the base and weld metals on samples repaired by welding using the scandium-containing filler metal.

Magnesium alloy Ml-10 was melted in an induction crucible furnace of the IPM-500 type by a commercial technology. Refining of the alloy was performed with flux VI-2 in a distributing furnace by portioned tapping of the melt, to which the Mg--Sc master alloy (90 % Mg, 10 % Sc) additives were introduced, and standard 12 mm diameter specimens for mechanical testing were charged into a sandy-argillaceous mould. The mechanical test specimens were heat treated in furnaces of the Bellevue and PAP-4M type under the following conditions: quenching from (415 ± 5) °C, holding for 15 h, cooling in air; aging at (200 ± ± 5) °C, holding for 8 h and cooling in air.

Tensile strength and elongation of the specimens were determined by using the P5 tensile-testing machine at room temperature, and long-time strength at different temperatures was determined by using the AIMA 5-2 tensile-testing machine on the 5 mm diameter specimens (GOST 10145–81). Metal microstructure was examined with the «Neophot-32» microscope after etching in an agent consisting of 1 % nitric acid, 20 % acetic acid, 19 % distilled water and 60 % ethylene glycol. Microhardness of structural components of the alloy was determined the Buehler microhardness meter under a load of 0.1 N. X-ray phase microanalysis was carried out with the JSM-6360LA electron microscope.

Chemical composition of investigated variants of the alloy met the requirements of GOST 2856--79, and was almost identical in the content of main elements.

Microstructure of alloy Ml-10, cast by the standard technology, after heat treatment consisted of δ-solid solution with eutectoid $\delta + (MgZr)_{12}Nd$, the latter having the form of spherical regions. Increase of concentration of the scandium modifier in the alloy was accompanied by increase of dimensions of the spherical eutectoid regions (Figure 3), whereas size of the δ-phase remained almost unchanged (Figure 4).

Heat treatment improved uniformity of the alloy structure owing to redistribution of elements between the axis and inter-axis spacings of dendrites, as well as additional alloying of the matrix due to diffusion of elements from boundary precipitates of the $(MgZr)_{12}Nd$ phase.

X-ray microanalysis showed that the spherical regions were rich mostly in zirconium, neodymium and scandium. In the modified alloy, the content of scandium in spherical precipitates of eutectoid $(MgZr)_{12}Nd$ was approximately 1.5--2 times higher than in the δ-solid solution.

Decomposition of eutectoid took place in the specimens tested at a temperature of 150–250 °C. Analysis of the alloy structure showed that, along with the decomposition of eutectoid, its dissolution in the matrix took place in the process of a long-time influence

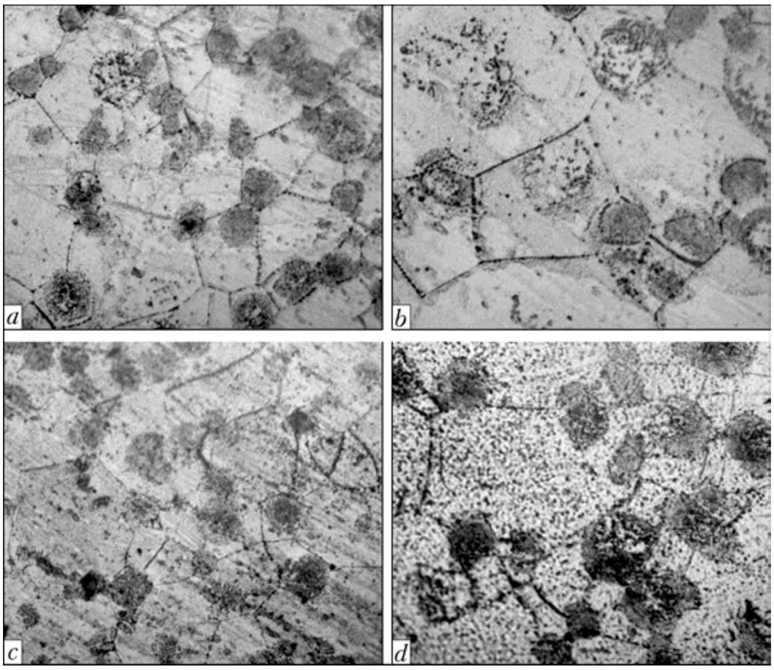

Figure 3. Microstructure (×500) of alloy Ml-10 without (*a, c*) and with scandium additive in an amount of 0.05 wt.% (*b, d*): *a, b* ---- after standard heat treatment; *c, d* ---- after tests at 150 °C (1252 h), and then at 250 °C (σ_t = 80 MPa)

by the test temperature, followed by precipitation of a fine intermetallic phase of the $(MgZr)_{12}Nd$ type with scandium (Figure 5). It was determined that fine intermetallic particles precipitated non-uniformly to form the regions of a dark streak pattern characterized by increased microhardness.

It was determined that the holding time at a specified temperature, as well as the presence of stresses, led to a more complete decomposition of the eutectoid phase. Coarsening of a structure caused by intensive precipitation of intermetallics, especially along the grain boundaries, took place at a temperature of 270 °C, which can explain a marked decrease in heat resistance of metal. Coarse boundary precipitates were detected in structure of the alloy containing 0.1 wt.% Sc. They promoted quick failure of the specimens during the long-time strength tests.

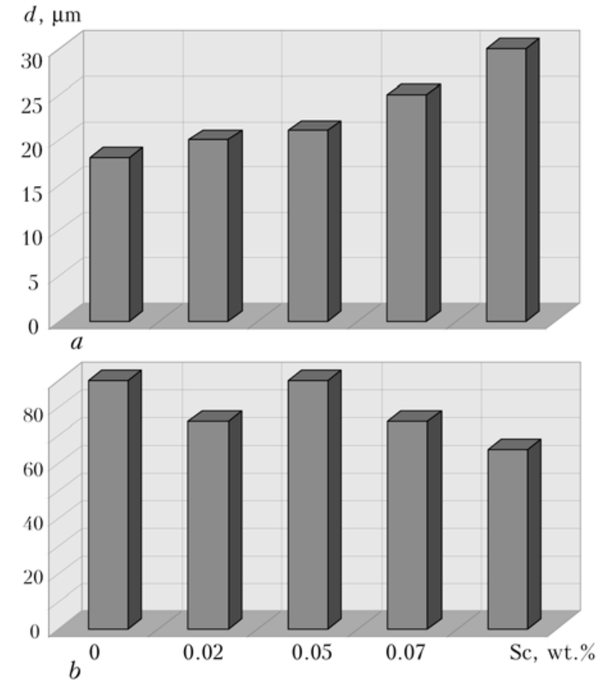

Figure 4. Change in size *d* of structural components of alloy Ml-10 at different scandium content: *a* ---- eutectoid $\delta + (MgZr)_{12}Nd$; *b* ---- δ-phase

Microhardness of δ-solid solution of the alloy without scandium, before heat treatment, was more than 3 times lower than microhardness of spherical eutectoids. After heat treatment, microhardness of the matrix increased, but that of the eutectoids decreased, this being indicative of an increase in the degree of uniformity of the alloy owing to heat treatment (Table 1). It can be seen from the Table that increase in scandium concentration of the alloy results in growth of microhardness of its structural components both before and after heat treatment.

Microhardness of the matrix and eutectoid increased with an increase of the test temperature from 150 to 250 °C, and microhardness of all the phases

Figure 5. Microstructure (×750) of alloy Ml-10 (0.07 wt.% Sc) with non-uniform precipitation of intermetallic phase after long holding (1252 h, σ_t = 80 MPa) at temperature of 150 °C

Table 1. Microhardness *HV* of structural components of Ml-10 alloy specimens

Sc content, wt.%	Matrix		Eutectoid	
	Before heat treatment	After heat treatment	Before heat treatment	After heat treatment
--	591.8--733.4	1017.3--1064.0	1821.6--2627.6	1225.5--1354.4
0.02	681.0--858.0	1114.1--1167.8	1891.6--3047.3	1286.6--1469.6
0.05	733.4--824.0	1017.3--1167.8	1891.6--2288.9	1287.5--1504.7
0.07	761.8--894.1	1114.1--1354.4	1781.6--2011.7	1589.5--1891.6
0.10	733.4--898.0	1167.8--1287.5	1781.6--2011.7	1589.5--1891.6

Table 2. Microhardness *HV* of structural components of Ml-10 alloy specimens after long-time strength tests (σ_t = 80 MPa) at different testing temperatures, °C

Sc content, wt.%	Matrix			Eutectoid		
	150	250	270	150	250	270
--	824.0--894.1	824.0--920.0	804.1--824.4	1026.0--1114.1	1114.5--1180.7	715.5--814.7
0.02	894.1--1064.0	894.1--1017.3	824.0--844.0	1114.1--1167.8	1167.8--1225.5	733.4--857.3
0.05	894.1--1017.3	894.1--1017.3	733.4--857.3	1114.1--1167.8	1167.8--1225.5	824.0--949.0
0.07	894.1--973.5	1064.0--1114.1	894.1--914.1	1114.1--1167.8	1167.8--1225.5	973.5--1167.8
0.10	894.1--973.5	1064.0--1114.1	894.1--914.1	1114.1--1167.8	1167.8--1225.5	973.5--1167.8

increased at a scandium content of the alloy equal to 0.05 wt.%. Increase of the test temperature of the investigated alloys to 270 °C resulted in some decrease of microhardness of the phases. However, the positive effect of scandium in the alloy on an increase of metal microhardness persisted (Table 2).

Thus, an addition of up to 0.07 wt.% Sc to alloy Ml-10 promoted some improvement of its mechanical and heat-resistant properties (Table 3). Further increase of the scandium content led to decrease of physical-chemical properties of metal.

Increase of the test temperature to 270 °C led to an almost 6 times reduction of the time to failure. Decrease in heat resistance of the investigated alloys at this temperature is caused by coarsening of the metal structure due to precipitation of intermetallics along the grain boundaries.

Table 3. Effects of scandium on mechanical properties and long-time strength (h, average value) of alloy Ml-10

Sc content, wt.%	σ_t, MPa	δ, %	Tests temperature T_{test}, °C, under loading (σ_t = 80 MPa)		
			150/250	250	270
--	235	3.6	1251.50/26.25	47.50	9.00
0.02	253	4.6	1252/56	53.16	11.16
0.05	245	6.3	1252/48.75	71.50	16.00
0.07	240	4.0	1252.5/64.0	61.80	12.60
0.10	232	3.5	1252.5/48.0	36.50	13.60
GOST 2856--79	≥ 226	≥ 3.0	--	--	--

Note. Long-time strength testing of specimens was carried out in steps ---- at 150 °C (numerator), and then at 250 °C (denominator).

Therefore, modifying of magnesium alloy Ml-10 by scandium provides the fine uniform structure. Improved mechanical properties and heat resistance of the alloy are achieved at a scandium content of 0.05--0.07 %.

To study weldability of metal after heat treatment, the Ml-10 alloy plates 200 × 100 × 10 mm in size were welded by using a filler in a form of cast samples measuring 8 × 200 mm, made from the same alloy with 0.06--0.07 wt.% Sc and without scandium. Then the cylindrical proportional samples 5 mm in diameter were manufactured (according to GOST 6996--66). Argon-arc welding was carried out with a tungsten electrode and experimental samples of the filler by using the TD-500 welding transformer, OSPP-3 oscillator, and PB-35 ballast rheostat. The quality of the weld was checked by the X-ray test method.

Structure of the base metal had a form characteristic of alloy Ml-10 in the heat-treated state, the weld metal consisted of the δ-solid solution and

Table 4. Effects of scandium on size *d* of structural components, microhardness *HV* and mechanical properties of welded specimens of alloy Ml-10

Sc content, wt.%	*d*, μm		*HV*	Mechanical properties	
	Matrix	Eutectoid		σ_t, MPa	δ, %
--	40--100 / 18--50	30--50 / 20--40	910.0 / 930.0	226--230	3.0--3.6
0.05--0.06	30--100 / 15--35	20--50 / 15--30	905.8 / 980.4	241--245	4.4--5.6

Note. Data on the base metal are given in numerator, and data on the weld metal are given in denominator.

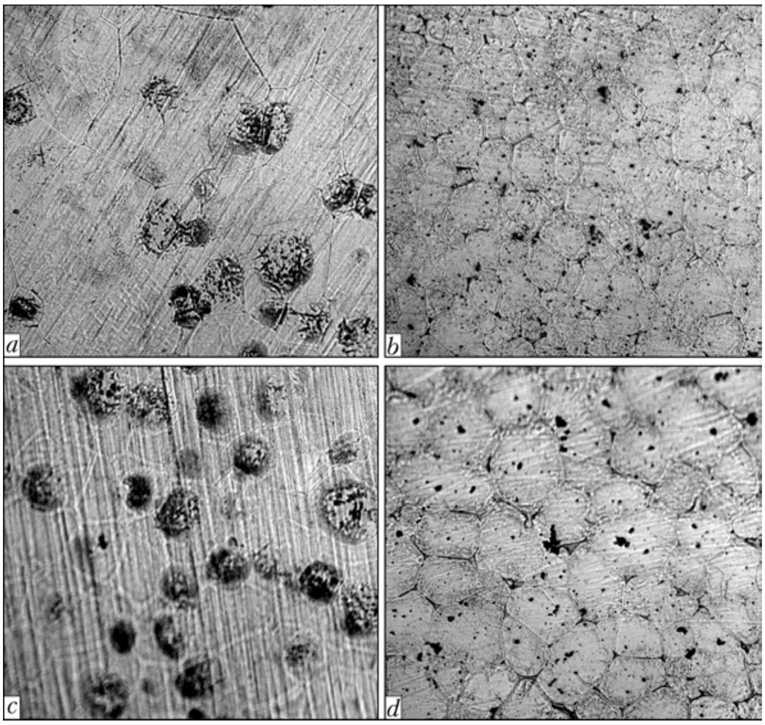

Figure 6. Microstructure (×500) of base (*a, b*) and weld metals (*b, d*) produced without (*a, b*) and with scandium addition (*c, d*)

$(MgZr)_{12}Nd$ phase situated along the grain boundaries in the form of light grey film precipitates (Figure 6).

Structural components of the weld metal were much smaller in size than those of the base metal (Table 4), and microhardness of the weld metal was somewhat higher than that of the base metal.

Mechanical properties of the scandium-containing Ml-10 alloy specimens were higher than without scandium. Failure of welded specimens during the tests came through the base metal or near-weld zone, but not through the weld.

Practical verification of the Ml-10 alloy filler metal with scandium gave positive results in welding repair of cases of the aircraft engines. X-ray inspection did not detect defects in welding repaired zones. As to the level of mechanical properties, the weld metal met requirements of the corresponding standards.

Therefore, it can be concluded that the content of 0.05–0.06 wt.% Sc in alloy Ml-10 provides improvement of mechanical properties and heat resistance of the latter. Welding repair of surface defects on the Ml-10 alloy parts with the scandium-containing filler metal provides the tight and uniform fusion zone due to formation of a fine-grained structure of the weld metal and improvement of its mechanical properties.

1. Krivov, G.A., Ryabov, V.R., Ishchenko, A.Ya. et al. (1998) *Welding in aircraft construction*. Kiev: MIIVTs.
2. Altman, M.B., Belov, A.F., Dobatkin, V.I. et al. (1978) *Magnesium alloys*: Refer. Book. Pt 2. Moscow: Metallurgiya.
3. Ishchenko, A.Ya., Labur, T.M. (1999) *Weldable aluminium alloys with scandium*. Kiev: KVITs.
4. Shalomeev, V.A., Tsivirko, E.I., Lisenko, N.A. et al. (2007) Mechanical and special properties of heat-resistant alloy Ml-10 with scandium. *Vestnik Dvigatelestroeniya*, **2**, 172–176.
5. Shalomeev, V.A., Tsivirko, E.I., Zhemanyuk, P.D. et al. *Magnesium-based cast alloy*. Pat. 25055 Ukraine. Publ. 25.07.2007.

FROM THE HISTORY OF WELDING

DEVELOPMENT OF INERT-GAS WELDING (Review)

A.P. LITVINOV
Priazovsky State Technical. University, Mariupol, Ukraine

The history of origination and development of inert-gas arc welding is considered. Its appearance was based on application of atomic-hydrogen welding and submerged-arc welding. The first TIG and MIG welding processes were developed at the beginning of the 1940s, and were applied in aluminium structure fabrication. In subsequent years, the methods for controlling metal transfer into the weld pool were developed, and different technologies for welding nonferrous metals and alloys were elaborated.

Keywords: *welding fabrication, arc welding, inert-gas welding, pulsed-arc welding, special steel, aluminium alloy, titanium alloy, TIG welding, MIG welding, aircraft and rocket engineering, engineering history*

Inert-gas arc welding currently is one of the most widely accepted processes of joining metals and alloys, and it is applied in fabrication of critical engineering constructions, operating under extreme conditions. Research, technology, industrial application and equipment are described in tens of monographs, in particular works summarizing the results of its introduction into the leading industries over many years [1–6]. However, the origins of this process still have not been determined, the authors of the first inventions, the development of which led to the modern TIG and MIG processes, have not been named, and the stages of development of this process have not been analyzed.

The purpose of this work is investigation of the origin and evolution of the main processes of inert-gas nonconsumable and consumable electrode welding.

The 1960–1970s, characterized by establishment of the foundations of nuclear engineering, aerospace engineering, advances in chemical engineering, supersonic aviation, necessitated development of new structural materials for products operating under extreme conditions: superhigh and superlow temperatures, high mechanical loads, aggressive medium and radiation exposure. This, in its turn, required development of the technology of reliable joining of the most advanced high-temperature and cryogenic alloys based on iron, aluminium, titanium, zirconium, tantalum, niobium, vanadium, hafnium, etc. Solution of this problem envisaged protection of the welding zone by inert gases (argon, helium, neon, krypton, xenon and radon), which practically do not react with metals, irrespective of the temperature of the latter, and are insoluble in most of the metals.

Use of inert gases for welding zone protection was proposed already at the start of the XX century. In particular, in 1918 G. Lincoln was granted US patent 1589017 for such an idea. In 1919 G.H. Hobart from General Electric proposed using helium as shielding gas [7], in 1926 patents for Heliarc and Argonarc processes were issued to F.K. Duers [8]. However, a satisfactory metal quality could not be achieved. At the same time at General Electric I. Langmuir developed atomic-hydrogen welding and P. Alexander continued improving it, using combustible and active gases [7, 9]. Development of aviation started making ever higher requirements to the quality of welded joints. There was an urgent need of implementation of ideas of inert gas shielding. Soon G. Hobart and P.K. Devers designed an acceptable torch for manual welding [10]. By mid-1930s Bernard Welding Equipment started improving the technologies of tungsten-electrode argon-arc welding (TIG) [11]. In 1935 P. Alexander under laboratory conditions achieved good shielding of the weld pool by inert gas [12, 13]. In Germany, similar to a number of other countries, where atomic-hydrogen welding was widely used, attempts were made to replace hydrogen by helium (1938) and argon (1941) with the same welding schematic. It is, however, non known, if a technology acceptable for practical application was developed [14].

Specialists of Dow Chemical Co (USA) tried to solve the problem of welding aluminium and magnesium alloys, applying consumable-electrode argon-arc welding (MIG), but it was not possible to eliminate burns-through. At the end of 1941 R. Meredith (Nortron Aircraft) developed the technology of TIG welding in argon at reverse polarity direct current, and then also at alternating current from an industrial frequency transformer with a high-frequency attachment (US patent 2274631 of 24.02.1942). In 1942 T.R. Piper, V.H. Pavlek and R. Meredith (Nortron Aircraft) developed the technology of tungsten-electrode welding in helium [15]. At the start of 1940s inert-gas welding attracted interest also in Great Britain (V.S. Devers, G.R. Handfort) [16]. The first result of the activity of the British Welding Research Association was introduction of MIG welding in construction of aluminium ship «Queen Elizabeth» led by P.T. Houldcroft [17].

In 1948 in the USSR at the Research Institute of Aviation Technologies (NIAT) A.Ya. Brodsky, A.V. Petrov and others developed the processes of TIG and MIG welding. In order to lower the technology cost, experiments were conducted on welding aluminium and magnesium alloys in commercial argon and of stainless and high-temerpature steels in an argon-nitrogen mixture [18, 19]. However, by the start of 1950s the technology of inert-gas welding of aluminium alloy items more than 10 mm thick did not provide a sufficiently good quality. The method of automatic semi-submerged arc welding developed in 1951 at the E.O. Paton Electric Welding Institute (D.M. Rabkin) turned out to be more effective [20]. In the USA a discussion was held on the possibility of a broad application of TIG welding, and absence of spatter, elimination of active fluorine- and chlorine-containing fluxes, visibility of the melting zone were noted [21]. By the end of 1950s TIG welding was already used in the USSR, USA and a number of other countries in fabrication of structures from high-alloyed steels, inconel, monel, copper, aluminium and their alloys [1–3, 22].

The spatter problem arose at replacement of the nonconsumable tungsten electrode by a consumable electrode. A satisfactory technology of consumable-electrode inert-gas welding — MIG welding — was developed at Air Reduction, New Jersey (US patent 2504688 of 06.04.1950). A technology of consumable-electrode welding of thin joints was also developed [23]. In 1950s research aimed at solving the spatter problems in electrode wire melting was deployed. A dependence of the modes of electrode metal melting and transfer on welding parameters was established: «jet» and «transition, critical», and «globular». At a comparatively high current density the jet transfer features a sufficient stability. In this case, however, it is difficult to weld thin metal without burns-through. At current lowering below the critical value, globular transfer developed, which was accompanied by spatter [24]. Problems of control of base metal melting and formation of a sound weld metal, widening the range of welded materials and thicknesses, as well as joining methods, were also solved [25–27]. At the end of 1950s PWI implemented the idea of melting control and reduction of electrode metal spatter at power supply to the process by high-ampere pulses of welding current and used the experience of studying pulse arc ignition gained by B.E. Paton in improvement of welding transformers and design of current modulation devices [28].

The possibility of control of electrode metal melting and transfer, as well as other characteristics was achieved by regulation of the process, current pulse parameters or change of instant power. At NIAT in 1960 A.V. Petrov and G.A. Slavin developed attachments to standard power sources and special power sources for pulsed-arc welding, which ensure a stable running of the process, at which a low-power pilot arc is maintained in the pauses between the pulses (USSR Author's Cert. 663956).

Development rates of inert-gas welding in 1960s were higher than those of development of other joining processes. Researchers were intensively searching for technologies of fabrication of complex engineering constructions from new alloys, improvement of process efficiency, melting coefficient, widening the range of welded thicknesses. By the middle of the decade the industry obtained the technology of welding non-ferrous metals and stainless steels from less than 1 mm thickness up to tens of millimeters; mechanized welding in different positions in space. Attachments to standard power sources and special sources were developed, which provided a stable running of the process, in which a pilot arc is maintained in the pauses between the pulses. Power sources and technology were developed for alternating current welding with superposition of pulses or a group of pulses with different parameters; adjustment of current pulse parameters, voltage or variation of instant power by a certain program or with self-correction (B.E. Paton, A.G. Potapievsky, P.P. Shejko, A.A. Alov, A.V. Petrov, G.A. Slavin, etc.) [29–34]. Similar processes were developed also in the USA, Great Britain, Japan, Germany, Italy and a number of other countries [35–37]. High-frequency current modulation (more than 25 s^{-1}) was used to control electrode metal transfer and stabilization of MIG welding process. Infralow modulation frequency (up to 2 s^{-1}) in combination with variation of amplitude value of current and current pulse shape allowed an even broader control of the arc penetrability, thermal cycle of welding and weld formation [38, 39].

To increase the heat input and improve MIG welding efficiency, several researchers simultaneously proposed the technology of welding by «hot wire» — due to the heat of current flowing through the electrode wire from a separate source or due to welding current at a considerable removal of the current supply from the electrode tip. At further development of this technique (applying additional heat to the welding zone) in 1970s K.A. Yushchenko at PWI studied the weldability and developed the technologies of automatic welding of high-strength cold-resistant steel: MIG with a preheated electrode and TIG with a filler; circumferential and longitudinal welds of equivalent strength were made [40]. TIG welding process ensured more stable parameters of the joint, precise maintenance of the penetration depth, ability of welding blanks of different thickness, while MIG welding was characterized by higher working speeds.

Improvement of the technologies of controlling melting of electrode materials and the pool was continued also in the subsequent years. TIG processes using pulsed current were also developed. For instance, it was proposed to lower the ratio of pulse current to pause current as metal heat conductivity becomes higher [41]. PWI developed the technology of improvement of formation, structure and strength properties of the welded joint by application of two-sided welding and transverse oscillations of the nonconsumable electrode [42, 43]. Transverse oscillations of the arc allowed reducing the dendritic inhomogeneity of the weld metal and the heat-affected zone. In 1959 TsNIITmash proposed welding by auto-pressing, in which after making a butt weld by nonconsumable electrode without a filler the weld is reinforced by multiple heating of the butt by the same arc, but with a lower heat input.

Despite the fact that inert-gas welding was appreciated primarily due to simplification of the problems with metallurgical processes, inevitable in submerged-arc and active-gas welding, searching for methods of metallurgical impact on the pool became one of the directions of investigation. Three directions formed: addition of active gases to the welding zone; application of fluxes and pastes; application of filler and electrode wires with additional compositions. At the same time, the same techniques were also used to control the physical processes in the welding zone — electrode melting and pool formation. In MIG welding addition of oxygen and carbon dioxide gas to argon in welding of carbon and some alloyed steels improves the weld metal density. A.V. Petrov (NIAT) developed a system of two-jet shielding in TIG welding: argon is fed through the inner nozzle and flows around the tungsten electrode, and carbon dioxide gas is fed through the outer nozzle. For welding items from highly reactive metals less than 1 mm thick NIAT developed a mixture of argon with 5–10 % hydrogen which allowed influencing the progress of metallurgical processes [2, 34]. Technologies of welding steel structures in a mixture of argon with 1–2 % oxygen at jet transfer of electrode metal were developed. Union Carbide Co determined the applicability of a mixture of 75 % argon and 25 % carbon dioxide in steel welding. A mixture of Ar (He) with «alloying gas» NO, O_2 or CO_2 was proposed for welding aluminium alloys [44]. Addition of small amounts of multicomponent additives of readily-ionized and surface-active substances, in particular, in metal wire guides was proposed for controlling the metallurgical processes [45].

In 1960s inert-gas welding was developing in one more direction — improvement of process penetrability. Processes were proposed, which are based on reduction of the active spot dimensions on the workpiece surface under the action of de-ionizing substances; arc column constriction (plasma-arc welding); bringing the electrode closer to the surface or its immersion into the weld pool (immersed-arc welding) and increased concentration of the arc energy at increase of external pressure.

In 1960s O.A. Maslyukov, A.N. Timoshenko (NIAT) established that MIG welding of titanium using oxygen-free fluoride-chloride fluxes improves the weld density (USSR Author's Cert. 183303, 183305). A considerable volume of priority research was performed at PWI. It was established that an increase of anode spot radius is observed in argon-arc welding of refined high-strength steel, produced by the processes of special electrometallurgy [46]. For constriction of the anode spot and increasing the current density it was proposed to add oxygen to the shielding gas, which is a surface active component, promoting an increase of pool fluidity, lowering of critical current of fine-drop transfer and improvement of weld formation [32]. PWI developed a process of TIG welding over a layer of oxygen-free fluxes and pastes with halide salts of alkali metals, which reduce the size of the active spot [47]. Increase of current density in the anode spot was attributed to lowering of conductivity of the arc peripheral region by fluoride vapours, decrease of cathode area size, as well as increase of the velocity of plasma flows in the arc and arc pressure on the anode, which results in concentration of the thermal flow, and lowering of the heat input [47–51]. These features of the process were used in welding of structures from molybdenum, niobium, special alloyed steels in rocket construction, nuclear power engineering, etc. Welding, which was called A-TIG, came to be regarded as one of the most promising, and is becoming applied in the counties of Europe, Asia and America [52–55].

The process of tungsten-electrode welding with constriction of arc column in the channel of small-diameter nozzle, proposed in 1957 by R. Gage, was named plasma welding [56]. Control of the thermal and dynamic head of the plasma-gas flow allowed widening the range of thicknesses being welded, also towards thickness reduction to fractions of a millimeter (microplasma welding) [57, 58]. Based on this idea at the start of 1960s NIAT, PWI and other organizations developed a number of techniques to improve the efficiency of tungsten-electrode welding. This process of TIG welding turned out to be the most promising for fabrication of critical aluminium structures, it is applied with different welding current pulses and methods of filler wire feed [59].

Immersed-arc welding turned out to be efficient for joining thick titanium alloys. With this process the tungsten electrode tip is below the surface of the parts being welded, and the arc gap is minimized [60, 61]. In TIG welding with two electrodes located in the plane normal to the weld axis, it was possible to increase the deposition factor and widen the range of adjustment of base metal penetration depth. Using the necessary filler materials (wire, etc.) this process allows producing a weld composition differing from the base metal, this being particularly necessary for cladding [62].

A significant effect was achieved when helium was used as shielding gas in straight polarity TIG welding of aluminium alloys. With this process the distance between the workpiece surface and the electrode is about 1 mm and the arc is actually completely immersed. As the arc running in helium evolves 1.5 to 2 times more energy than in argon, it as possible to achieve deeper penetration at lower preheating of base metal, increase the welding speed and reduce the HAZ. Despite a comparatively high cost of helium and complexity of performance (electrode tip sharpening to an acute angle and arc length in the range of 1–2 mm) the process became applied in welding workpieces from heat-hardenable aluminium alloys in aircraft and rocket construction and in shipbuilding [63, 64]. To some extent, the effectiveness of TIG welding remains to be high enough, when a mixture of argon (35–40 %) and helium is used.

Inert-gas welding continues developing at the end of XX–start of XXI centuries. In this period the efforts are focused on development of technologies providing an increase of process efficiency, achieving a high quality of joints on new alloys, broadening the range of the produced structures, etc. In addition, work on assessment of the electromagnetic impact on the electrode and the pool, combining the heat sources (combined and hybrid processes) becomes more intensive.

Gas-shielded arc welding acquires the image of a process characterized by broad capabilities of automation and robotization of the processes of manufacturing various-purpose products, making welds of different geometry in all the positions in space.

CONCLUSIONS

1. Processes of inert-gas arc welding began to be developed in 1940s, which was due to the arising demands of fabrication of high-quality critical structures from non-ferrous metals and special steels. Inert-gas nonconsumable-electrode (TIG) and consumable-electrode (MIG) arc welding became extensively developed in the USA, Great Britain and the USSR.

2. Experience of application of atomic-hydrogen welding, control of the processes of electrode melting in submerged-arc welding formed the scientific-technical basis for development of the new welding process. Pulsed-arc processes ensured the high quality of the deposited metal.

3. Welding in inert gases and gas mixtures was developing along the path of improvement of electrode metal transfer and weld formation control, widening the range of welded alloys and workpieces and lowering the power content.

1. Brodsky, A.Ya. (1956) *Argon tungsten-arc welding*. Moscow: Mashgiz.
2. Petrov, A.V. (1961) *Technology of inert-gas arc welding*: Refer. Book. Ed. by E.V. Sokolov. Vol. 2. Moscow: Mashgiz.
3. Russo, V.L. (1962) *Inert-gas arc welding of aluminium alloys*. Leningrad: Sudpromgiz.
4. (1985) *Metals science of aluminium alloys*. Ed. by S.T. Kishkin. Moscow: Nauka.
5. (1985) *Current problems of welding nonferrous metals*: Proc. of 11th All-Union Conf. Kiev: Naukova Dumka.
6. Welson, R.A. (1961) Vapor-shielded arc welding at 200 imp. *Welding J.*, **1**, 13.
7. Langmuir, I. (1923) The pressure effect in gaseous discharge. *J. Franklin Institute*, **11**, 751–762.
8. (1969) An industry in retrospect 50 year progress. *Welding J.*, **4**, 165--169.
9. Alexander, P.P. (1928) Stability of the welding arc. *J. AIEE*, **3**, 48--53.
10. Campbell, W.J. (1946) The selection of welding processes. *Welding J.*, **8**, 704--706.
11. Bernard, A. (1966) Living pioneers. *Ibid.*, **12**, 62--63.
12. Alexander, P.P. (1932) Welding high carbon steel. *J. AWS*, **2**, 8.
13. West, E.G. (1985) Aluminium welding in this century. In: *The centenary of modern welding, 1885--1985*. London: Welding Inst.
14. Mair, H. (1997) Entwicklung und Bedeutung technischer Gase in der Schweisstechnik. In: *100 Jahre DVS*. Berlin.
15. Piper, T.R. (1942) Heliarc welding. *Welding J.*, **11**, 770--772.
16. Shanley, F.R., Fallon, C.T. (1946) Discussions on the heliarc welding process as applied in the aircraft industry. *Ibid.*, **1**, 32.
17. Houldcroft, P.T. (1952) The assembly of the aluminium alloy superstructure of them. Pt 1: «Queen Elizabeth». *Weld. and Metal Fabr.*, **6**, 228--229.
18. Maslov, G.A. (1948) To results of the meeting on welding operations in aircraft industry. *Avtogennoe Delo*, **2**, 32--33.
19. Brodsky, A.Ya. (1948) Argon-arc welding of thin metals. *Ibid.*, **10**, 11--17.
20. Rabkin, D.M. (1953) New method of automatic welding of aluminium. *Avtomatich. Svarka*, **4**, 45--50.
21. Berryman, J. (1950) For inert gas shielding argon or helium? *Iron Age*, **3**, 155--157.
22. Rabkin, D.M., Gurevich, S.M., Bugrij, F.S. (1950) *Welding of nonferrous metals*. Kiev: Mashgiz.
23. Diebold, J.M. (1946) Fusion welding of sheet metal. *Welding J.*, **8**, 724--732.
24. Needham, J.C., Cooksey, S.J., Milner, P.R. (1960) Metal transfer in inert gas-shielded arc welding. *British Welding J.*, 7(**2**), 101--104.
25. Petrov, A.V. (1954) Consumable-electrode inert-gas arc welding of stainless steels. *Vestnik Mashinostroeniya*, **9**, 68–70.
26. Petrov, A.V. (1955) Fusion of electrode wire in argon-arc welding. *Svarochn. Proizvodstvo*, **2**, 4--7.
27. Dyatlov, V.I. (1964) Elements of electrode metal transfer theory in electric arc welding. In: *New problems of welding technique*. Kiev: Tekhnika.
28. Paton, B.E., Zavadsky, V.A. (1954) Pulsed ignition of arc with the purpose of considerable lowering of welding transformer voltage. *Avtomatich. Svarka*, **4**, 46--62.
29. Paton, B.E. (1963) Further development of systems of automatic control and regulation of welding processes. *Ibid.*, **5**, 1--6.
30. Paton, B.E., Potapievsky, A.G., Podola, N.V. (1964) Consumable electrode pulsed arc welding with programmed regulation of the process. *Ibid.*, **1**, 1--6.
31. Paton, B.E., Shejko, P.P. (1965) Transfer control in consumable electrode arc welding. *Ibid.*, **5**, 1--7.
32. Gurevich, S.M., Zamkov, V.N., Kushnirenko, N.A. (1965) Increase in penetration efficiency of titanium alloys during argon-arc welding. *Ibid.*, **9**, 1--4.
33. Alov, A.A., Shmakov, V.M. (1962) Argon-arc welding with additional argon flow. *Svarochn. Proizvodstvo*, **3**, 13--16.
34. Petrov, A.V., Slavin, G.A. (1966) Study of technological possibilities of pulsed arc. *Ibid.*, **2**, 1--4.
35. Terry, C.A., Tyler, W.T. (1958) Inert-gas tungsten-arc welding. *Weld. and Metal Fabr.*, **2**, 58--61.
36. Needham, J.C., Carter, A.W. (1965) Material transfer characteristic with pulsed current. *Welding J.*, **5**, 229.
37. Trindade, E.M., Allum, C.J. (1984) Characteristics in steady and pulsed current GMAW. *Weld. and Metal Fabr.*, **9**, 264--272.
38. Shigaev, T.G. (1983) Methods of welding current modulation and devices for their implementation. *Avtomatich. Svarka*, **8**, 51--55.
39. Wilson, J.L., Claussen, G.E., Jackson, C.E. (1956) The effect of I^2R heating on electrode melting rate. *Welding J.*, **1**, 1--8.
40. Yushchenko, K.A., Pustovit, A.I. (1979) Welding of high-strength cold-resistant steel 03Kh12N10MT. *Avtomatich. Svarka*, **1**, 55--56.
41. (1980) Survey on the application of pulsed currents with the TIG process. *Welding in the World*, **3/4**, 61--66.
42. Mandelberg, S.L., Gordonny, V.G. (1961) Single-sided two-layer argon-arc welding of alloy steel plate. *Avtomatich. Svarka*, **9**, 18--23.
43. Makara, A.M., Kushnirenko, B.N. (1967) Transverse displacements of the arc as a factor of improvement of welded joint structure. *Ibid.*, **1**, 31–35.
44. Iversen, K., Schellong, B. (1983) Vielfach die bessere Loesung Wolframinertgasschweissen von Aluminium mit wechselnder Polung. *Praktiker*, **9**, 400, 402.
45. Paton, B.E., Voropaj, N.M. (1979) Activated consumable electrode shielding-gas welding. *Avtomatich. Svarka*, **1**, 1–7, 13.
46. Makara, A.M., Mosendz, N.A. (1971) *Welding of high-strength steels*. Kiev: Tekhnika.
47. Savitsky, M.M., Leskov, G.I. (1980) Mechanism of the influence of electronegative elements on arc penetrability with tungsten electrode. *Ibid.*, **9**, 17--22.
48. Simonik, A.G., Petviashvili, V.I., Ivanov, A.A. (1976) Contraction effect of arc discharge at introduction of electronegative elements. *Svarochn. Proizvodstvo*, **3**, 49--51.
49. Ostrovsky, O.E., Kryukovsky, V.N., Buk, B.B. et al. (1977) Effect of activated fluxes on penetrability of the welding arc and energy concentration in the anode spot. *Ibid.*, **3**, 3--4.
50. Paton, B.E., Zamkov, V.N., Prilutsky, V.P. et al. (2000) Arc contraction by flux in tungsten-electrode argon-arc welding. *Avtomatich. Svarka*, **1**, 1--8.
51. Yushchenko, K.A., Kovalenko, D.V., Kovalenko, I.V. (2001) Application of activators for TIG welding of steels and alloys. *The Paton Welding J.*, **7**, 37--43.
52. Lucas, W. (2000) Activating flux ---- improving the performance of the TIG process. *Weld. and Metal Fabr.*, **2**, 7--10.
53. Gordon, J.R. (1995) Perspectives on welding research and development in the USA. *Welding Review Int.*, **8**, 95--106.
54. (2001) Welding and joining technologies in XXI century. *J. JWS*, 70(**3**), 6--18.
55. Zamkov, V.N., Prilutsky, V.P. (2004) Theory and practice of TIG-F (A-TIG) welding (Review). *The Paton Welding J.*, **9**, 11--14.
56. Gage, R.M. (1960) The plasma-arc torch: a new research tool. *Electric Manufacture*, **1**, 144--146.
57. Dudko, D.A., Lakiza, S.P. (1960) About new possibilities of welding with high-temperature arc constricted by gas flow. *Avtomatich. Svarka*, **11**, 38--46.
58. (1979) *Microplasma welding*. Ed. by B.E. Paton. Kiev: Naukova Dumka.
59. Dudko, D.A., Kornienko, A.N. (1968) Welding of aluminium-magnesium alloys by AC plasma arc. In: *Cutting, surfacing and welding by constricted arc*. Moscow: TsIINTI-Neftekhimmash.
60. Dolotov, B.I. (2004) Welding with immersed tungsten electrode. *Mashinostroenie*, **1**, 20--24.
61. Blashchuk, B.E., Boeva, G.E., Langer, N.A. (1985) Application of argon-arc welding with electromagnetic stirring in manufacturing chemical apparatuses from titanium alloys. In: *Current problems of nonferrous metals*. Kiev: Naukova Dumka.
62. Zamkov, V.N., Topolsky, V.F., Kushnirenko, N.A. (1978) Tungsten-electrode double-arc welding of plate titanium. *Avtomatich. Svarka*, **2**, 44--47.
63. Rabkin, D.M., Ivanova, O.N., Steblovsky, B.A. et al. (1971) Welding of aluminium alloys at straight polarity direct current. *Ibid.*, **3**, 71--72.
64. Budnik, V.P., Steblovsky, B.A., Buzko, M.G. (1982) Penetrability of DC and AC arc. *Ibid.*, **8**, 68--71.

ELECTROHYDRAULIC-PULSED TREATMENT FOR STRENGTHENING THE SURFACES OF 110G13MLS STEEL FROGS

N.A. ONATSKAYA and **L.Yu. DEMIDENKO**
Institute of Pulse Processes and Technologies, NASU, Nikolaev, Ukraine

The case of samples of point frogs from austenitic steel 110G13MLS was used to demonstrate the possibility of strengthening the surfaces of wear-resistant steels by jet electrohydraulic-pulsed treatment. It is determined that 1.4 times increase of hardness of the surface of a steel sample is caused by microplastic deformation of the sliding and twinning type developing in it. This results in increase of wear-resistance of the steel surface layer.

Keywords: *electrohydraulic-pulsed treatment, austenitic high-manganese steel, wear resistance, surface strengthening, generator of high-velocity jets, microplastic deformation, hardness*

It is well known that in most cases the performance of equipment parts is determined by wear resistance of their working surfaces. As the costs of repair and maintenance of the equipment related to wear resistance exceed several times their initial costs [1], increase of wear resistance of machine and apparatus parts is of high importance for extension of their service life. As a rule, fracture of machine parts, equipment and structural components begins from the surface during operation. Consequently, strengthening of the surface layers of parts is of a decisive importance in terms of extension of their life time. Respectively, strengthening of metal surfaces is a hot and critical problem of modern production.

Different technological methods are used in engineering practice for strengthening of the part surfaces. Most of them are based on plastic and thermoplastic deformation of relatively thin surface volumes of the parts, and maintaining of their core unchanged.

Study [2] shows that an electrohydraulic-pulsed treatment (EGPT) with a high-velocity liquid jet, which is directed normal to the treated surfaces of the welded samples of aluminium-manganese alloys, allows not only reducing tensile stresses in the weld, but also making them compressive, equal to the initial stresses in absolute value. In this case an increase of 23 % in metal hardness takes place along the weld axis. This suggests that such a treatment can be used for strengthening of the surfaces of metal parts made, for example, from wear-resistant steels working under wearing conditions.

The aim of this study was to investigate the possibility of application of high-velocity liquid jets, generated by a high-voltage discharge in a small-volume chamber, for strengthening of the surfaces of parts made from wear-resistant steels. In this case, energy of the electric discharge is accumulated in a liquid accelerated by the high-velocity jet generator. It gains a velocity comparable with or higher than the velocity of sound in liquid. The pressure of drag of the jet developing in this case amounts to $1\cdot10^9$ Pa, i.e. it becomes comparable with the dynamic yield stress of the majority of structural materials [3].

To check such a possibility, the choose was made of high-manganese austenitic steel 110G13MLS, which is widely used in different braches of industry, in particular, in mining and mineral production, agricultural and transport machine-building industry [4]. As a rule, the surfaces of 110G13MLS steel parts are strengthened by affecting it with impact or high specific static pressures.

Point frog samples measuring 100 × 50 × 20 mm, made from the above steel, were selected as an object of investigations. Mechanical properties of the steel in the initial state are as follows: tensile strength σ_t = = 800 MPa, yield stress σ_y = 400 MPa, and hardness HV 2100 MPa. Jet EGTP* was carried out normal to the sample surfaces at discharge energy W_0 = 20 kJ. Liquid jets were generated in a rigid chamber with a capacity of 250 cm^3, having a cone nozzle (angle at the cone vertex is equal to 60°) and outlet of 8 mm diameter. The air gap from the outlet of the chamber to the surface of water was h = 40 mm, the jet velocity measured with the help of high-speed filming using the VFU-1 device amounting to 1500 m/s.

The maximum pressure of the jet on a barrier at the moment of its deceleration was determined from the results of measuring of the velocity of the liquid jet by using a relationship given in study [2]. As shown by the calculations, in this case it was 2180 MPa. Thus, jet EGTP provides an intensive effect of liquid on a material. Moreover, it does not deteriorate quality of the treated surface. Immersion

*Jet EGTP as well as measurement of jet velocity were carried out by engineer Yurchenko E.S.

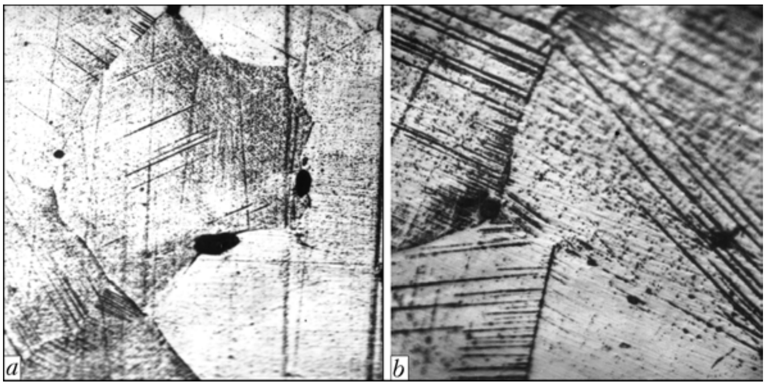

Microstructure (×500) of steel 110G13MLS before (*a*) and after treatment with a high-velocity liquid jet (*b*)

of the surface to a depth of 0.7 mm takes place as a result of the liquid jet effect.

The results of measurement of hardness of the treated part surfaces show that its value is equal to *HV* 5200 MPa, which corresponds to *HB* 4700 MPa. This is more than 2 times in excess of the value of their hardness before the treatment, and 1.4 times in excess of that required for increase of wear resistance [4]. The depth of the hardened metal layer of the treated surface was 0.25 mm. Apparently, to increase the depth of hardened surface layer it is necessary to change geometric sizes of the jet generator or increase the discharge energy, as they exert the major effect on the velocity of a liquid flow and, hence, on the pressure of the jet at the moment of its collision with the barrier. As increase of the energy is not always appropriate, the required depth of hardened surface layer can be achieved due to increase of the quantity of pulses.

As shown by metallographic examinations, the structure of the steel surface layer, which was identified before the treatment as austenitic with a small amount of spherical carbides located along the boundaries of austenite grains (Figure, *a*), after the effect by the liquid jet was characterized by formation of microplastic deformation of the sliding and twinning type (Figure, *b*). The deformation occurred mainly along one sliding system, which is the evidence of the presence of hardening. No refinement of austenite grains was fixed in this case.

CONCLUSIONS

1. The possibility is shown of applying liquid jets generated by a high-voltage discharge in a small-volume chamber for hardening of metallic surfaces of parts made from wear-resistant steels.

2. The value of hardness of the surfaces of parts made from high-manganese steel 110G13MLS is 1.4 times higher after treatment with high-velocity jets than that required for improvement of their wear resistance.

3. The results obtained are indicative of the potential possibility of commercial application of the said type of treatment for hardening of the surfaces of parts made from manganese steel 110G13MLS.

1. Pronikov, A.S. (1978) *Reliability of machines*. Moscow: Mashinostroenie.
2. Merin, B.V. (1985) *Electrohydraulic treatment of machine-building parts*. Leningrad: Mashinostroenie.
3. Kudinov, V.M., Petushkov, V.G., Yurchenko, E.S. et al. (1987) Jet electrohydraulic-pulsed treatment of welded joints. *Avtomatich. Svarka*, **8**, 73–74.
4. Davydov, N.G. (1979) *High-manganese steel*. Moscow: Metallurgiya.

THESIS FOR A SCIENTIFIC DEGREE

NTUU «Kiev Polytechnic Institute»

On December 12, 2008, **A.I. Bushma** (the E.O. Paton Electric Welding Institute of the NAS of Ukraine) defended Thesis for Scientific Degree on «Modeling the processes of interaction of laser radiation with dispersed materials in laser and hybrid laser-plasma coating».

The thesis is dedicated to investigation of the processes of laser and hybrid laser-plasma coating, development of physico-mathematical models of laser and combined (laser-plasma) heating of particles of the dispersed materials, and determination, on this basis, of new methods for control of the spraying particles thermal characteristics. A theory was developed in the thesis to explain interaction of laser radiation with fine-dispersed particles, which applies to coating conditions by using lasers. Formulas for calculation of the characteristics of absorption and dispersion of laser radiation by the spraying particles were derived on the basis of solution of the problem of diffraction of the electromagnetic wave at a non-uniformly heated spherical particle. It is shown that in the case when the particle size is comparable with the wavelength, a significant non-uniformity of spatial distribution of the electromagnetic energy absorbed by the particle takes place. For metallic particles this energy dissipates within the range of a thin skin-layer (surface heat source), whereas in the case of ceramic particles it dissipates in the whole volume of the particle (distributed heat source).

The thesis suggests a mathematic model of laser and laser-plasma heating of particles of dispersed materials. It shows that laser heating of ceramic particles is characterized by a significant non-uniformity of the temperature field and, consequently, of optical properties of the particle material. This results in a change of integral characteristics of scattering and absorption of radiation in the process of heating of a particle, as well as distributed characteristics of heat generation in its volume, which can be accompanied by thermal explosion of the particle. The possibility is proved of controlling the temperature field of spraying particles due to an adequate combination of volume (laser) and surface (plasma) heating, which is important for spraying of materials with low thermal conductivity.

The thesis presents the developed mathematic model of the processes of moving and heating of separate particles under the conditions of laser, plasma and hybrid spraying of ceramic coatings. Calculation of temperature fields for the SiO_2 particles sprayed by using the argon plasma jet, CO_2-laser beam and their combination showed significant dependence of the time-spatial distribution of temperature in the particles on the spraying method. The suggested model is generalized for a case of accounting for dispersion and absorption of the laser beam by the whole set of the spraying particles. It is shown that the consumption of powder has a significant influence on distribution and integral characteristics of the beam, as well as on a thermal state of the SiO_2 particles in spraying by using CO_2-laser.

The author of the thesis proposed a design of and made an experimental model of the integrated indirect-action laser-arc plasmatron intended for coating. The plasmatron is based on the combined laser-arc discharge formed at a co-axial combination of the focused CO_2-laser beam and constricted (plasma) arc. Testing of the plasmatron showed high stability of its operation in an arc current range of 20–200 A and beam power of up to 4 kW. Investigations of technological capabilities of the plasmatron evidence perspective of its application for spraying various powder materials and deposition of diamond and diamond-like coatings.

NEWS

FLUX-CORED WIRE FOR WELDING OF PIPES WITH A FORCED WELD FORMATION

The flux-cored wire MegafilR 715B-A for welding with a forced weld formation under field conditions was developed by enterprise «Arcsel» (Donetsk, Ukraine) together with the company «Drahtzug Stein Wire & Welding» (Germany). It has an air-tight sheath and does not require preliminary calcination before application even under the site conditions and pipeline construction at the increased humidity of surrounding air. The wire has a flux core of a basic type, that in combination with a traditional low content of diffusion-movable hydrogen in the deposited metal enables providing perfect mechanical properties of metal of circumferential welds of pipes welded by the position welding.

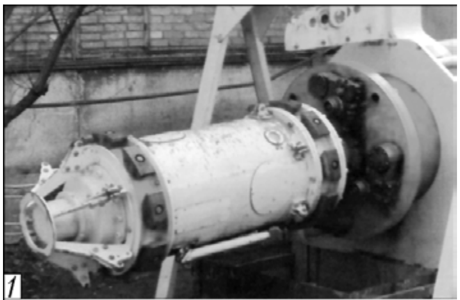
1


2

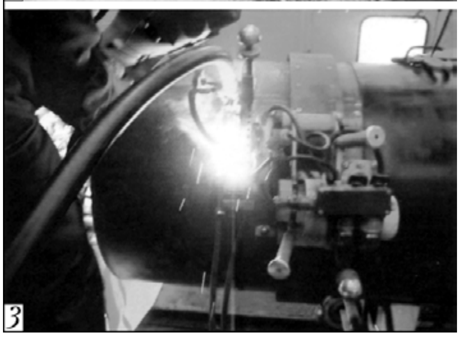
3

The wire is used in technology of high-efficient one-sided welding of position joints of pipes under the site conditions, developed by «Neftegazstrojizolyatsiya». The equipment set for realization of technology includes a sleeve for edge preparation *1* and a self-propelled aligning device with a copper backing ring *2*, providing matching of edge joining operations and installing a backing forming ring, allowing the performance of one-sided welding of position joints using flux-cored wire without preliminary root welding and tacks. Here the pipes with wall thickness up to 10 mm can be welded for one pass providing the required mechanical properties of metal of weld and welded joint as a whole.

A simple welding head *3* of a unique design and small weight provides the performance of pipe joint welding using the flux-cored wire MegafilR 715B-A at the speed twice faster on average than that in welding using shielding gas and rutile flux-cored wire with a free weld formation and in 3–4 times faster than in welding using covered electrodes. The flux-cored wire MegafilR 715B-A is serially produced at the enterprise «Arcsel» and recommended for welding of position joints of pipes in complex with equipment of enterprise «Neftegazstrojizolyatsiya» for edge preparation and welding under the site conditions and pipeline construction under any climatic conditions. The guarantee period of wire storage in dry warehouse is 24 months. The possible period of use of welding flux-cored wire MegafilR 715B-A at the site without any additional preparation before welding at the absence of direct ingress of moisture on the wire is one month.